Alkalinity sources in the Dutch Wadden Sea

Mona Norbisrath[1,2,3], Justus E. E. van Beusekom[1], & Helmuth Thomas[1,2]

[1]Institute of Carbon Cycles, Helmholtz-Zentrum Hereon, Geesthacht, 21502, Germany

[2]Institute for Chemistry and Biology of the Marine Environment (ICBM), Carl von Ossietzky University Oldenburg, Oldenburg, 26129, Germany

[3]now at: Department of Marine Chemistry and Geochemistry, Woods Hole Oceanographic Institution, Woods Hole, MA, 02543, USA

Correspondence to: Mona Norbisrath (mona.norbisrath@whoi.edu)

Abstract

Total alkalinity (TA) is an important chemical property playing a decisive role in the oceanic buffering capacity of CO_2. The oceanic buffering capacity total alkalinity (TA), as the major global CO_2 sink, is of growing scientific interest. TA is mainly generated by weathering on land, and further by various anaerobic metabolic processes in water and sediments. The Wadden Sea, located in the southern North Sea is hypothesized to be a source of TA for the North Sea, but quantifications are scarce. This study shows observations of ed TA, dissolved inorganic carbon (DIC), and nutrients in the Dutch Wadden Sea in May 2019. Along several transects, surface samples were taken to investigate spatial distribution patterns and to compare them with data from the late 1980s. A tidal cycle was sampled to further shed light on TA generation and potential TA sources. We identified the Dutch Wadden Sea as a source of TA with an average TA generation of 7.6 µmol TA kg^{-1} h^{-1} TA during ebb tide in the Ameland Inlet. TA was generated in the sediments with deep pore water flow during low tide enriching the surface water. A combination of anaerobic processes and $CaCO_3$ dissolution were potential sources of TA in the sediments. We deduce assume that seasonality and the associated nitrate availability in particular influence TA generation by denitrification, which we assume is low in spring and summer.

1 Introduction

As the regulator of the ocean carbon dioxide (CO_2) sink, total alkalinity (TA) is of increasing scientific interest and is investigated worldwide in the so called "Anthropocene" (Abril and Frankignoulle, 2001;Bozec et al., 2005;Chen and Wang, 1999;Dickson, 1981;Middelburg et al., 2020;Norbisrath et al., 2022;Renforth and Henderson, 2017;Thomas et al., 2004;2009;Sabine et al., 2004). The "Anthropocene" describes the current era of our planet, when environmental changes, driven by humans, have become identifiable in geological records (Zalasiewicz et al., 2010;Crutzen, 2002). One of the most threatening changes for our climate is the anthropogenic driven increase in atmospheric greenhouse gases (GHG), such as CO_2. To counteract the increasing atmospheric CO_2 concentrations and the ongoing climate warming, a combination of several

30 pathways is needed. Beside a strict reduction of CO_2 emissions, also net-negative emissions are required, which capture the

31 atmospheric CO_2 and store it either based on land or in the ocean (e.g., Keith et al., 2006;Matthews and Caldeira, 2008;Zhang

32 et al., 2022). The climate and the increasing atmospheric CO_2 content is also naturally regulated by the open ocean, and around

33 a quarter of the global anthropogenic CO_2 emissions are already removed by it (Friedlingstein et al., 2022). The carbon storage

34 capacity of the North Sea is an important atmospheric CO_2 sink as it exports the absorbed CO_2 in the deep layers of the Atlantic

35 Ocean where it is stored on longer time scales (Borges et al., 2005;Bozec et al., 2005;Burt et al., 2016;Brenner et al., 2016;Hu

36 and Cai, 2011;Schwichtenberg et al., 2020;Thomas et al., 2004;2009). Two important aspects of the oceanic climate regulation

37 are the oceanic circulation and TA. TA, primarily consisting of bicarbonate and carbonate, is generated by chemical rock

38 weathering (Suchet and Probst, 1993;Meybeck, 1987;Berner et al., 1983), and in various stoichiometries by calcium carbonate

39 ($CaCO_3$) dissolution and anaerobic metabolic processes, such as denitrification, which is the reduction process of nitrate to

40 dinitrogen gas in the nitrogen cycle (Hu and Cai, 2011;Wolf-Gladrow et al., 2007;Chen and Wang, 1999;Brewer and Goldman,

41 1976). Since TA, CO_2 uptake and its export to the deep ocean are mainly disentangled in the open ocean, TA and the oceanic

42 circulation interact closely in highly active and shallow ocean areas such coastal zones and continental and marginal shelves.

43 ~~The climate and the increasing atmospheric CO_2 content is mainly regulated by the open ocean. Around 30 % of the global~~

44 ~~anthropogenic CO_2 emissions are removed by the ocean (Gruber et al., 2019). The carbon storage capacity of the North Sea is~~

45 ~~an important atmospheric CO_2 sink as it exports the absorbed CO_2 in the deep layers of the Atlantic Ocean where it is stored~~

46 ~~on longer time scales (Borges et al., 2005;Bozec et al., 2005;Burt et al., 2016;Brenner et al., 2016;Hu and Cai,~~

47 ~~2011;Schwichtenberg et al., 2020;Thomas et al., 2004;2009).~~

48 ~~Two important aspects of the oceanic climate regulation are the oceanic circulation and TA. Both interact well in highly active~~

49 ~~and shallow ocean areas such coastal zones and continental and marginal shelves.~~ In these shallow areas, TA is ~~very~~ susceptible

50 to changes due to various metabolic processes and the influence of adjacent zones like rivers, estuaries, marshes, and tidal flats

51 (e.g., Norbisrath et al., 2022;2023;Wang et al., 2016;Voynova et al., 2019). A previous study by Norbisrath et al. (2022)

52 showed that an enhanced riverine, metabolic alkalinity would lead to increasing CO_2 absorption in the coastal zones of the

53 North Sea, highlighting the need to further investigate TA regulation in adjacent zones of coastal oceans.

54 Coastal zones, which are the direct interface between most, if not all, compartments of the Earth system (i.e., atmospheric,

55 terrestrial, aquatic, and oceanic) and human societies, appear particularly vulnerable to environmental and climate change

56 (Glavovic et al., 2015). This holds true for the Wadden Sea, the shallow, coastal sea along an approximately 500 km coastline

57 of the Netherlands, Germany, and Denmark, in the southern North Sea, which is declared as an UNESCO world natural heritage

58 site since 2009. Most of the Wadden Sea is located between the protecting barrier Islands and the Mainland, which makes it

59 the world's largest uninterrupted stretch of tidal flats with multiple tidal inlets (Fig. 1). Due to the topography, the Wadden

60 Sea is a highly dynamic ecosystem with influences from the mainland and the North Sea (Hoppema, 1993;Postma, 1954;van

61 Raaphorst and van der Veer, 1990). Driving forces of the biogeochemical dynamics in the Wadden Sea are nutrient ~~and organic~~

62 ~~matter (OM)~~ imports by rivers and high suspended particulate matter (SPM) and organic matter (OM) imports from the North

63 Sea (van Beusekom et al., 2019;van Beusekom et al., 2012;Postma, 1954). Physical sources of variability in the Wadden Sea

are oceanic driven wind, waves, and tidal currents, as well as the counterclockwise circulation of the North Sea (Elias et al., 2012). Large tidal amplitude and currents in conjunction with shallow water depths allow for vertical water column mixing and an exchange between the pelagic and benthic realms including deep pore water exchange (Røy et al., 2008). The strong~~high~~ tidal currents also impact the biogeochemistry of the North Sea (Postma, 1954), as they cause an exchange of water between the North Sea and the Wadden Sea and play an important role in the import of particulate matter from the North Sea (Burchard et al., 2008).

~~TA, primarily consisting of bicarbonate and carbonate, is generated by chemical rock weathering (Suchet and Probst, 1993;Meybeck, 1987;Berner et al., 1983), and in various stoichiometries by calcium carbonate ($CaCO_3$) dissolution and anaerobic metabolic processes, such as denitrification, which is the reduction process of nitrate to dinitrogen gas in the nitrogen cycle (Hu and Cai, 2011;Wolf-Gladrow et al., 2007;Chen and Wang, 1999;Brewer and Goldman, 1976). Understanding of TA sources have recently become increasingly important due to increasing anthropogenic CO_2 emissions, and the resulting demand for ocean-based net negative CO_2 emissions (e.g., Keith et al., 2006;Matthews and Caldeira, 2008;Zhang et al., 2022). In~~ pPrevious studies identified, the Wadden Sea ~~was identified~~ as a TA source for the North Sea with a loading between 39 Gmol yr^{-1} (Schwichtenberg et al., 2020) and 73 Gmol yr^{-1} (Thomas et al., 2009). Both studies suggested the entire Wadden Sea as one of the most important TA sources of the carbon storage capacity for the North Sea. Burt et al. (2016) highlighted the importance of coastal TA production for regulating the buffer system in the North Sea, and suggested denitrification as the major TA source. Due to the strong connection between the North Sea and the Wadden Sea, a better understanding of TA generation in the latter is required. Here, we focus on the Dutch Wadden Sea that has been well-studied during the past decades (Hoppema, 1990, 1991, 1993;De Jonge et al., 1993;Elias et al., 2012;Ridderinkhof et al., 1990;Postma, 1954;van Beusekom et al., 2019;Schwichtenberg et al., 2017). In particular Hoppema (1990);(1993) observed the spatial and temporal variability of TA in May in the late 1980s, which we compare with our observed transect data to detect potential differences over the last 30 years. In addition, we further discussed ~~shed light on~~ potential TA sources in the Dutch Wadden Sea.

2 Methods

2.1 Study site and sampling

This study is based on samples collected on a research cruise (LP20190515) in the Dutch Wadden Sea (Frisian Islands) on RV *Ludwig Prandtl* in May 2019 (Fig. 1). We collected water samples in the Wadden Sea starting at Harlingen, through the Vlie Inlet along ~~around~~ the islands Vlieland and Terschelling, through the Ameland Inlet to Ameland Island, from there on via the Frisian Inlet to Lauwersoog, and around Schiermonnikoog Island via the Ems-Dollard Inlet to Emden. In addition, we sampled a half tidal cycle during ebb tide (from high tide to low tide) on ~~(~~21 May ~~.05.~~2019. To set the range of ebb tide data in relation, we also sampled a half tidal cycle during flood tide (from low tide to high tide) on 23 May 2019 for comparison.~~) and from low tide to high tide (23.05.2019)~~ Both half tidal cycles were sampled ~~on each day~~ as an anchor station in the waterway at the western side of Ameland in the Ameland Inlet on each day.

96 Nearly half-hourly, we ~~continuously~~ collected discrete surface (1.2 m depth) water samples with a bypass from the onboard

97 flow-through FerryBox system (Petersen et al., 2011), which also provided essential physical parameters such as salinity and

98 temperature.

99 For TA and DIC measurements we sampled water with overflow into 300 mL BOD (biological oxygen demand) bottles and

100 preserved them with 300 µL saturated mercury chloride solution ($HgCl_2$) to stop biological activity. Each BOD bottle was

101 filled without air bubbles and closed by using a ground-glass stopper coated in Apiezon® type M grease and a plastic cap. The

102 samples were stored in a cool dark environment until measurements in the lab.

103 Water for nutrient samples was filtered through pre-combusted (4 h, 450 °C) GF/F filters and the filtrate was stored frozen in

104 three 15 mL Falcon tubes for triplicate measurements in the lab.

105 To determine the total carbon (C), organic carbon (C_{org}) and nitrogen (N) concentrations in SPM and associated C_{org}:N ratios,

106 we used pre-combusted (4 h, 450 °C) GF/F filters, which were dried after sampling at 50 °C to remove all humidity and were

107 stored frozen afterwards until measurement.
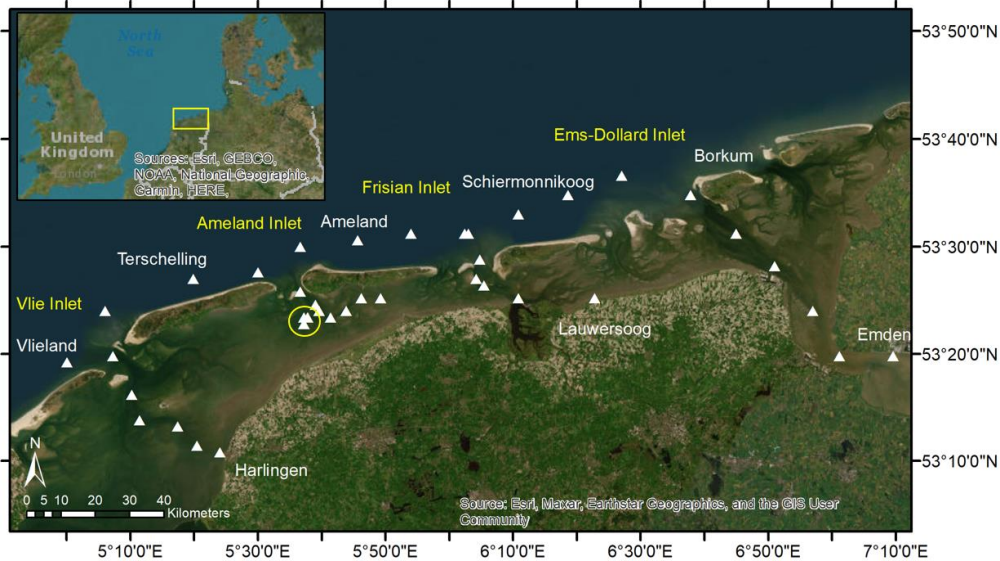
108

109 **Figure 1** Sampling site in the Dutch Wadden Sea. The sampling stations around the Frisian Islands in May 2019 are visualized

110 with white triangles. The yellow circle highlights the anchor stations for the tidal cycle sampling in the Ameland Inlet on two

111 days. During the sampling day from low tide to high tide, we had two samples that we took slightly more western due to

112 drifting. The island and city names are shown in white, the inlets in yellow. The tidal flats and sedimentary structures are well

113 visible between the barrier islands and the mainland.

2.2 Carbon species analyses

The parallel analyses of TA and DIC were carried out in March 2020 by using the VINDTA 3C (Versatile INstrument for the Determination of Total dissolved inorganic carbon and Alkalinity, MARIANDA - marine analytics and data), which measures TA by potentiometric titration and DIC by coulometric titration both with a measurement precision < 2 µmol kg^{-1} (Shadwick et al., 2011). To ensure a consistent calibration of both measurements, cCertified reference material (CRM batch # 187) provided by Andrew G. Dickson (Scripps Institution of Oceanography) was measured before and after the samples and used used. to ensure a consistent calibration of both measurements.

The calcite and aragonite saturation states (Ω) and the pH were computed with the CO$_2$SYS program (Lewis and Wallace, 1998), using the measured parameters TA, DIC, salinity, temperature, silicate and phosphate as input variables, together with the dissociation constants from Mehrbach et al. (1973), as refit by Dickson and Millero (1987).

2.3 Nutrient analyses

The nutrients were measured with a continuous flow automated nutrient analyzer (AA3, SEAL Analytical) and a standard colorimetric technique (Hansen and Koroleff, 2007) for nitrate (NO$_3^-$), nitrite (NO$_2^-$), phosphate (PO$_4^{3-}$), and silicate (Si), and a fluorometric method (Kérouel and Aminot, 1997) for ammonium (NH$_4^+$) (Grasshoff et al., 2009). The nutrient samples were measured against reference materials VKI SW4.1B (NO$_x$, NO$_2$ and NH$_4$) and VKI SW4.2B (Si and PO$_4$) in July 2019. The maximum standard deviations were 0.322 µmol L^{-1} for NO$_3^-$, 0.014 µmol L^{-1} for NO$_2^-$, 0.081 µmol L^{-1} for NH$_4^+$, 0.014 µmol L^{-1} for PO$_4^{3-}$ and 0.165 µmol L^{-1} for Si.

For the C$_{org}$ determination, filters were acidified with 1N HCl and dried overnight to remove all inorganic carbon content. Filters were measured with a CHN-elemental analyzer (Eurovector EA 3000, HEKAtech GmbH) in the Institute of Geology, University Hamburg, and calibrated against a certified acetanilide standard (IVA Analysentechnik, Germany). The standard deviations were 0.05 % for carbon and 0.005 % for nitrogen.

2.4 Data analyses

The data analyses were performed by using RStudio Version 1.3.1073 © 2009-2020 RStudio, PBC. The linear regression Model II was performed by using the "lmodel2" R package, and the plots were created with the "ggplot2" R package.

3 Results

3.1 Spatial parameter distribution

To investigate the spatial distribution of total alkalinity (TA) in the Dutch Wadden Sea and compare its general status with earlier studies (in particular Hoppema, 1990), we observed the spatial distribution of TA and related parameters in surface water along a transect from the coastal mainland towards the open North SeaNorth Sea as a surface water transect.

143 The temperatures varied between 12 and 16 °C with higher temperatures towards the coastal mainland (Fig. 2a).

144 We identified two main sub regions based on the salinity values. First the Ems-Dollard Inlet, which showed salinities lower

145 than 28 and with the minimum value of 20.25 at the most upstream station. And second, around Ameland Island and the

146 remaining of our investigated region in the Dutch Wadden Sea with salinities showing ~~Salinity was relatively stable with~~ only

147 minor differences varying from 28 to 33 (Fig. 2b). ~~Lower salinities were only observed in the four sampling stations in the~~

148 ~~Ems Estuary with the minimum value of 20.25 at the most upstream station.~~

149 Spatial transect TA concentrations ranged from 2332 µmol TA kg^{-1} to 2517 µmol TA kg^{-1}. We observed lower concentrations

150 on the ~~oceanic, i.e.,~~ North Sea side of the Frisian Islands with somewhat higher concentrations around Ameland (Fig. 2c). In

151 contrast to the North Sea~~oceanic~~ side, the values were higher (> 2380 µmol TA kg^{-1} ~~TA~~) in the Wadden Sea. ~~Only i~~In the Ems-

152 Dollard Inlet ~~Estuary~~, the concentrations were even higher, with values up to 2517 µmol TA kg^{-1} ~~TA~~ at the most upstream

153 station. ~~Higher TA values in the Wadden Sea than in the open ocean, supporting the assumption of TA being generated in this~~

154 ~~tidal flat area.~~

155 Silicate (Si)~~, showed a similar pattern with~~ higher concentrations in the Wadden Sea and lower ones towards the North Sea

156 ~~ocean~~ (Fig. A1a). Highest concentrations were observed at the coastal mainland and in the Ems-Dollard Inlet ~~Estuary~~. Silicate

157 concentrations ranged~~were~~ between 0.3~~2~~6 and 56.3~~2~~ µmol Si L^{-1}. Both, the calcite and aragonite saturation states (Ω) were

158 supersaturated in the entire study region~~site~~. Saturation state v~~V~~alues ranged from 2.3 to 4.6 for calcite (Fig. A1b), and from

159 1.4 to 3.0 for aragonite (Table B1). Highest values were observed at the North Sea side ~~oceanic side~~ of the barrier islands ~~in~~

160 ~~the North Sea. T~~, and ~~he~~ lowest values ~~were observed~~ near Harlingen and in the Ems-Dollard Inlet ~~Estuary~~. Like the calcite

161 and aragonite saturation states, the pH values were higher in the North Sea, and lower in the Wadden Sea and near the coastal

162 mainland (Fig. A1c). The pH values ranged from 7.86 to 8.19, and~~.~~ ~~The~~ lowest values were observed near Harlingen and in

163 the Ems-Dollard Inlet ~~Estuary~~. The nitrate (NO$_3^-$) concentrations were in a ~~similarly~~ low range (< 3 µmol NO$_3^-$ L^{-1} ~~NO$_3^-$~~)

164 throughout the ~~transect~~study region. Higher concentrations (< 6 µmol NO$_3^-$ L^{-1} ~~NO$_3^-$~~) were observed only at a few stations

165 close to land, and maximum concentrations (< 38 µmol NO$_3^-$ L^{-1} ~~NO$_3^-$~~) were observed in the Ems-Dollard Inlet ~~Estuary~~ (Fig.

166 A1d). DIC concentrations ranged from 2097 µmol DIC kg^{-1} to 2430 µmol DIC kg^{-1} (Fig. A1e). DIC values showed a similar

167 pattern as TA values, with higher concentrations near the coastal mainland and in the Ems-Dollard Inlet ~~Estuary~~, and

168 decreasing concentrations toward the North Sea, where DIC reached minimum values.

169
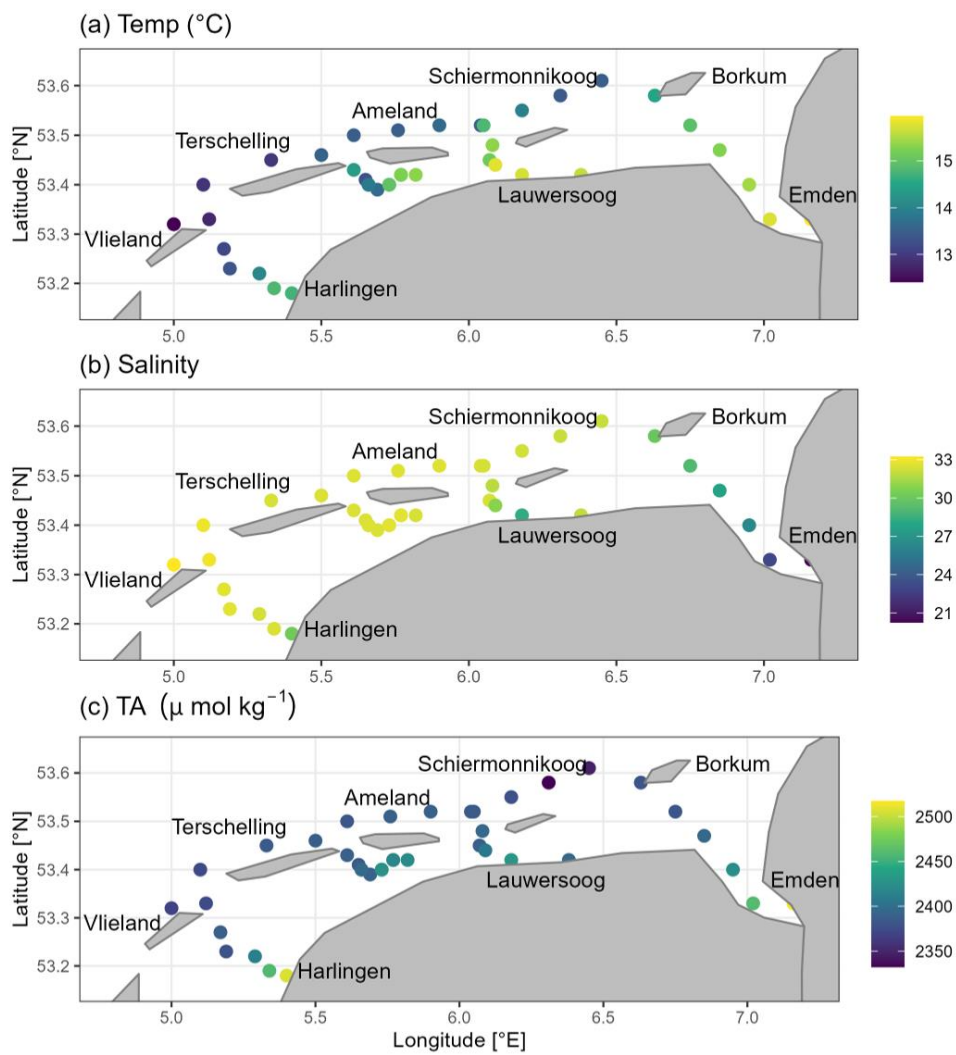
Figure 2 ~~Spatial~~ ~~Latitudinal and longitudinal~~ distribution of a) temperature (°C), b) salinity, and c) total alkalinity (TA; µmol

kg⁻¹) from surface water samples in May 2019.

172

173 Compared to the other transects of this study region, Tthe strong influenceimpact offrom the inner Ems Estuary is visible at the

174 most upstream station in the Ems-Dollard Inlet in all parameters, showing lowest pH and calcite saturation state values, and

175 highest values of TA, DIC, nitrate, silicate and phosphate. with higher values in the outer estuary and its adjacent zones, or

176 with lower values in case of pH and the calcite saturation state. Furthermore, we observed higher values around Ameland

177 Island than in the western part of the transect starting from Harlingen towards the Vlie Inlet. At the oceanic The outer side of

178 the Vlie Inlet reflects, the impact of the North Sea conditions with is visible through lower temperatures and higher salinities.

179 The North Sea impact is also visible in the mixing plot between TA and salinity (Fig. 3). A relatively lStatistical significant

180 linear mixing behavior was only observed in the transect through the Ems-Dollard Inlet ($R^2 = 0.81$) and through the Vlie Inlet

181 ($R^2 = 0.77$), where TA concentrations decreased with increasing salinities from the mainland towards the North Sea ocean

182 (Fig. 3)., identifying the Dutch Wadden Sea as a source of TA. Whereas in the Ems-Dollard Inlet mixing is dominated by

183 riverine water with high TA concentrations, the mixing in the Vlie Inlet showed a more prominent mixing of Wadden Sea and

184 North Sea water. The TA concentrations in the Vlie Inlet and around Ameland, both at the North Sea side (Ameland NS) and

185 the Wadden Sea side (Ameland WS) were higher than the TA concentration computed for the salinity end-member in the Ems-

186 Dollard Inlet, suggesting the Dutch Wadden Sea as a source of TA (Fig. 3). Both the Ameland NS and WS data clearly indicated

187 a non-conservative behavior with a range of TA concentrations at near constant salinities.

188 In contrast to the TA concentration computed for the salinity end-member in the Ems-Dollard Inlet, we detected higher TA

189 concentrations around Ameland, both at the North Sea side (Ameland NS) and the Wadden Sea side (Ameland WS), as well

190 as in the Vlie Inlet, which further support additional TA sources in the Wadden Sea (Fig. 3). The Ameland NS and Ameland

191 WS data clearly indicated non-conservative behavior with increasing TA concentrations at constant salinities.

Formatiert: Hochgestellt

Formatiert: Hochgestellt

192
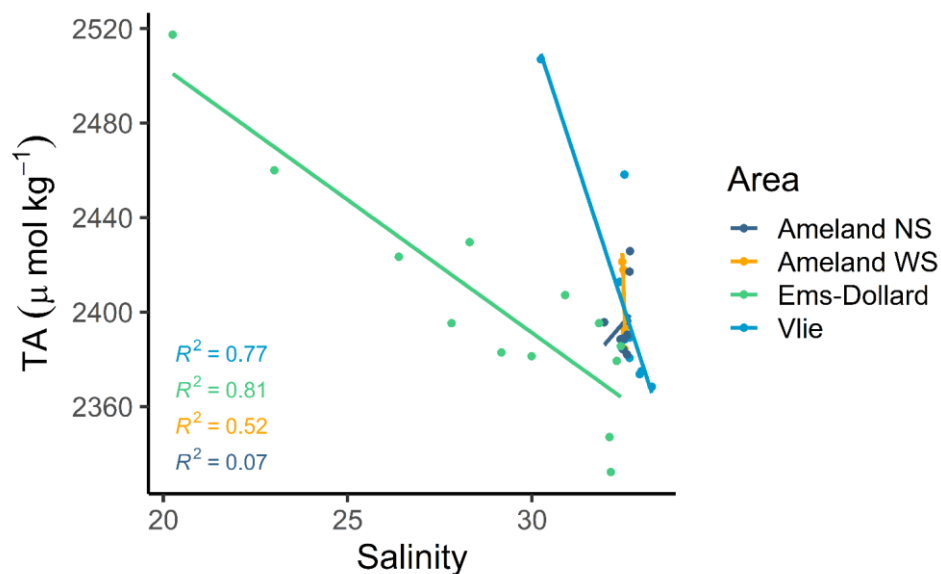
Figure 3 Mixing plot of ~~between~~ total alkalinity (TA) and salinity in the ~~oceanic~~ North Sea side of Ameland and the Frisian
Inlet (Ameland NS), in the Wadden Sea site of Ameland (Ameland WS), around Schiermonnikoog and in the Ems-Dollard
(Ems-Dollard) Inlet, and in the Vlie Inlet (Vlie).~~.~~

3.2 Tidal cycle

~~To estimate TA generation in the Dutch Wadden Sea, to shed light on potential TA sources, and to estimate the potential TA~~
~~amount that is exported to the North Sea, w~~We observed a half tidal cycle at an anchor station in the Ameland Inlet ~~on two~~
~~days during flood tide and~~ during ebb tide, ~~respectively~~to 1) identify potential TA sources and 2) to quantify potential TA
export to the North Sea. ~~Here, the focus is on ebb tide data that w~~We ~~used to~~ identif~~ied~~y patterns in ~~the~~ several biogeochemical
parameters in ~~off running~~ water leaving the tidal flats (Fig. 4, Table B1). Temperature increased from 13.25 to 14.7 °C (Fig.
4a). The salinity observations allow us to exclude addition by mixing with freshwater sources, since the ~~s~~Salinity was constant
~~around~~ between 32.5~~0~~ and 32.52 (Fig. 4b, Table B1), which is in the range of southern North Sea water excluding admixture
of local fresh water sources. ~~Salinity values were in the range of saline waters like water of the North Sea.~~

During ebb tide, TA ranged from 2387 µmol TA kg^{-1} during high tide to 2438 µmol TA kg^{-1} during low tide (Fig. 4a). We observed an increase of 51.6 µmol TA kg^{-1} (ΔTA) during ebb tide (6.8 h), resulting in a TA increase of 7.6 µmol TA kg^{-1} h^{-1} at the sampling location.

DIC concentrations behaved similar to TA with minimum values at high tide (2172 µmol DIC kg^{-1}), and maximum values (2273 µmol DIC kg^{-1}) at low tide, resulting in an increase of 101.3 µmol DIC kg^{-1} (ΔDIC) or 14.9 µmol DIC kg^{-1} h^{-1} (Fig. 4b). DIC increased almost twice as much as TA.

Nitrate slightly increased during ebb tide by 0.92 µmol NO$_3^-$ L^{-1} (ΔNO$_3^-$) from a minimum of 1.26 µmol NO$_3^-$ L^{-1} to a maximum of 2.17 µmol NO$_3^-$ L^{-1} (Fig. 4e), resulting in a nitrate increase of 0.13 µmol NO$_3^-$ L^{-1} h^{-1}.

Silicate showed a similar pattern with low values (1.8 µmol Si L^{-1}) at high tide during ebb tide to a maximum of 11.2 µmol Si L^{-1}, resulting in a silicate increase (ΔSi) of 9.4 µmol Si L^{-1} or 1.4 µmol Si L^{-1} h^{-1} during ebb tide (Fig. 4d).

Ammonium increased from 3.47 µmol NH$_4^+$ L^{-1} to 6.22 µmol NH$_4^+$ L^{-1} during ebb tide (Fig. 4g), resulting in an ammonium increase (ΔNH$_4^+$) of 2.74 µmol NH$_4^+$ L^{-1} or 0.4 µmol NH$_4^+$ L^{-1} h^{-1}.

The calcite and aragonite saturation states had maximum values (Ω_{Ca} = 3.8, Ω_{Ar} = 2.4) at high tide and decreased to their minimum (Ω_{Ca} = 3.1, Ω_{Ar} = 2.0) during ebb tide (Fig. 4h,i, Table B1). The influence of the North Sea is indicated by the observed maximum at high tide, which decreased during the ebb.

Like omega, the maximum pH was 8.07 at high tide and decreased to a minimum (7.93) during ebb tide (Fig. 4g).

C_{org}:N ratios of SPM increased during ebb tide (Fig. 4h). A minimum C_{org}:N ratio of 5.6 was observed around high tide and increased to a maximum of 13.0 during ebb tide. Simultaneously, the SPM concentration increased during ebb tide, from 12.8 mg SPM L^{-1} to a maximum of 82.4 mg SPM L^{-1} at the second last station (Table B1).

232
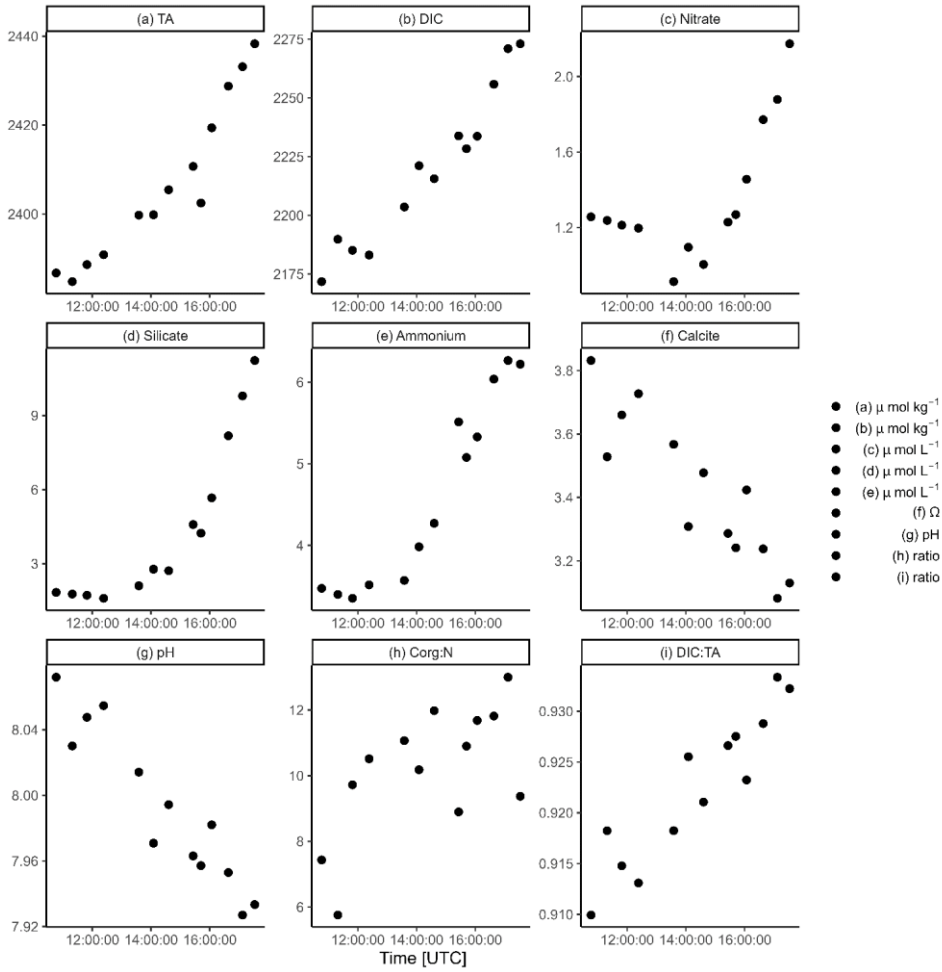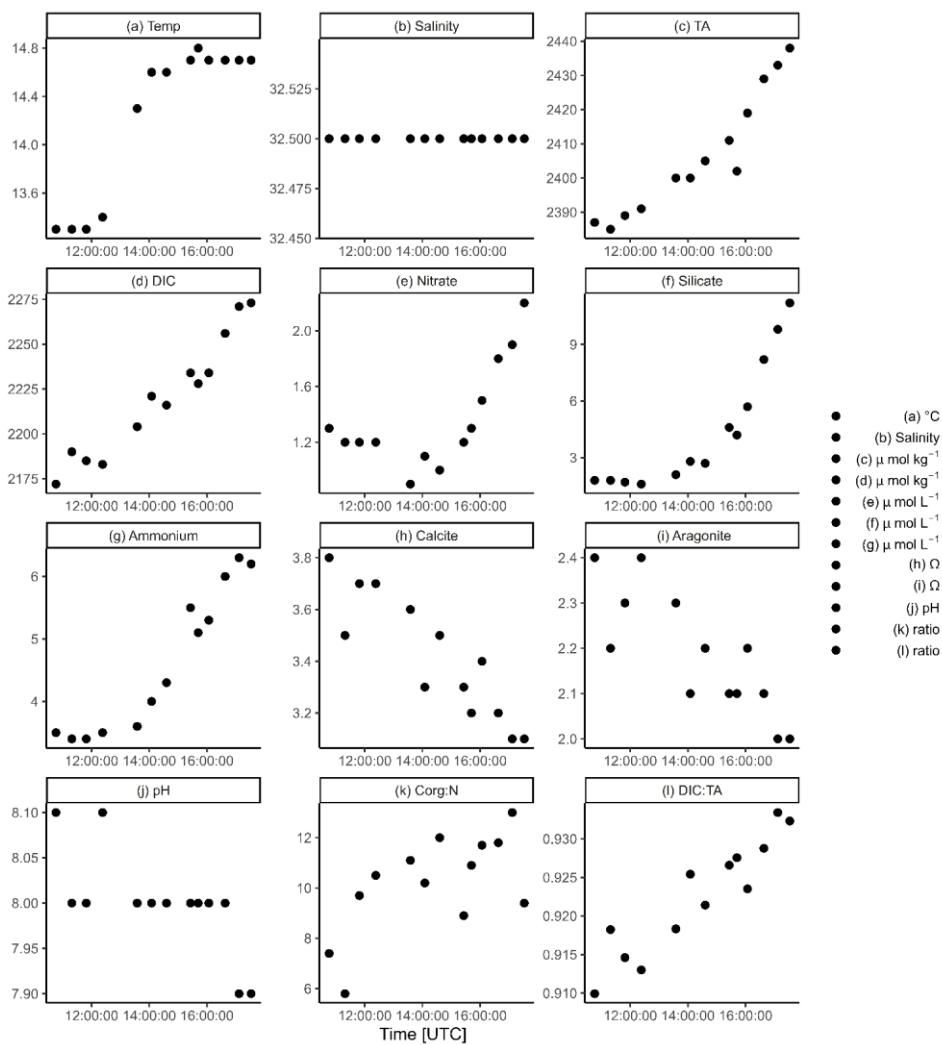
Figure 4 A half ~~T~~tidal cycle from high tide to low tide. Temporal distribution of a) temperature, b) salinity, c) total alkalinity

(TA),~~d~~b) dissolved inorganic carbon (DIC),~~e~~c) nitrate,~~f~~d) silicate,~~g~~e) ammonium,~~h~~f) calcite saturation state (Ω), i)

235 aragonite saturation state (Ω), ~~i~~g) pH, ~~k~~h) C_{org}:N ratio of SPM, and ~~l~~i) DIC:TA ratio. Note the different y-axes and the +1

236 hour time difference between the local time and the UTC time. ~~.~~

3.3 TA generation

238 Tidal forcing leads to a bi-diurnal exchange between ~~The Dutch~~ Wadden Sea ~~is exposed to strong tidal forcing by the~~ and

239 North Sea water~~leading to a bi-diurnal exchange of water~~. The ~~strong~~ tidal forcing also induces a strong benthic-pelagic

240 coupling (Huettel et al., 2003;Røy et al., 2008). Many studies support that the outflowing water exports material from the

241 sediment including remineralization products from organic matter (e.g., Billerbeck et al., 2006;Røy et al., 2008). Here, we

242 focus on the hypothesis that the sediments are a significant source of TA ~~To support our assumption of a sediment source of~~

243 ~~TA, we further investigated potential TA sources.~~

244 For a first rough estimate of a maximum TA export during ebb tide, we used the mean observed TA increase (ΔTA / 2) of

245 25.8~~51.6~~ µmol TA kg^{-1} ~~TA~~ during ebb tide (in the Ameland Inlet, part of the Borndiep tidal basin), ~~and~~ the tidal prism of 478

246 $\times 10^6$ m^3 of the Borndiep tidal basin, and a share of intertidal flats of 53 % ~~Ameland Inlet~~ (Louters and Gerritsen, 1994).

247 Assuming that only the interdidal sediments exchange TA, we estimated a TA export of 6.6 Mmol TA per tide to the North

248 Sea. Assuming two ebb tides and a lunar cycle of 24.8 hours this would result in a daily export of 12.7 Mmol TA. ~~With this~~

249 ~~estimate, we obtained a rough TA export on the order of 23.9 mol TA during ebb tide from the Ameland Inlet into the North~~

250 ~~Sea. With a tidal duration of 6.8 h, the estimated TA export of 23.9 mol would result in a TA export of 3.5 mol h^{-1} TA.~~

251 ~~Based on the~~The significant correlation of TA and silicate ($R^2 = 0.93$), and ~~on~~ the insignificant ~~nonlinear~~ relation between

252 ~~both,~~ TA and salinity ($R^2 = 0.32$), as well as silicate and salinity ($R^2 = 0.21$), suggest that ~~we were able to determine whether~~

253 TA originates from the tidal flats in this part of the Dutch Wadden Sea and is not from admixture carried ~~or is carried~~ by river

254 runoff. The significant correlation between TA and silicate both during ebb tide ~~Both TA and silicate increased almost~~

255 ~~proportionally during ebb tide,~~ pointing to the same source ~~origin~~ (Fig. 5b). ~~The non-conservative behavior of TA over salinity~~

256 ~~and silicate over salinity rules out any sources due to freshwater dilution and river runoff (Table B1).~~

257 To further elucidate potential TA sources in the Dutch Wadden Sea, we correlated TA with DIC, silicate, nitrate, and

258 ammonium in the half tidal cycle from high tide to low tide, respectively (Fig. 5). ~~The first four samples on the left side of the~~

259 ~~plots in Fig. 5 show values probably at the tipping point of high tide, whereby we recommend neglecting these samples in the~~

260 ~~interpretation of ebb tide samples.~~

261 The correlation between TA and DIC is a measure between anaerobic and aerobic processes. Our data show a strong positive

262 correlation between DIC and TA ($R^2 = 0.93$) with TA concentrations being higher than DIC concentrations (Fig. 5a). We

263 observed a release excess of DIC compared to TA as indicated by the slope of 1.89 and by an increase in DIC (ΔDIC = 101.3

264 µmol kg^{-1}) almost twice as high as TA (ΔTA = 51.6 µmol kg^{-1}) (Fig. 5a).

265 ~~First, the correlation between TA and DIC reveals the ratio between anaerobic and aerobic processes, which identifies a strong~~

266 ~~positive correlation between DIC and TA ($R^2 = 0.93$) with TA concentrations higher than DIC concentrations (Fig. 5a).~~

267 ~~However, even with concentrations of TA higher than DIC, the slope of 1.87 indicated DIC release excess with an increase in~~

268   ~~DIC (ΔDIC = 101.3 µmol kg^{-1}) almost twice as high as TA (ΔTA = 51.6 µmol kg^{-1}) (Fig. 5a).~~ This excess DIC may be caused

269   by strong CO_2 production due to high aerobic OM degradation, or by uptake from the atmosphere due to water movement by

270   tidal forcing. However, given the heterotrophic nature of the Wadden Sea (e.g., van Beusekom et al., 2012), a CO_2

271   undersaturation is unlikely. The TA increase can be fueled by various processes which we will discuss below. We detected ~~an~~

272   ~~almost~~ linear positive correlation of increasing TA and silicate (R^2 = 0.93) during ebb tide, supporting ~~the~~ pore water outflow

273   (Fig. 5b) as pore water is the major Si source during summer (van Bennekom et al., 1974). A stronger influence of the pore

274   water with ongoing ebb tide is indicated by increasing values. The positive correlation between nitrate and TA (R^2 = 0.67)

275   (Fig. 5c) was less strong than the correlations between TA and DIC, and TA and Si, which could be traced back on an effect

276   of the first four samplings points that were probably at the tipping point from high tide to low tide. ~~as mentioned above.~~ In the

277   remaining samples, the increasing nitrate and TA concentrations suggest a stronger ~~effect of~~ TA generation than nitrate

278   production, balancing TA that may be consumed by nitrification (i.e., nitrate production).
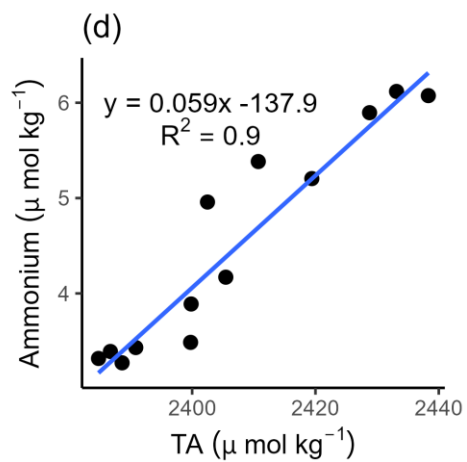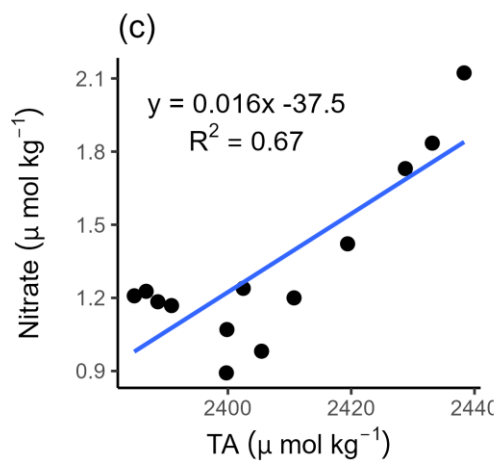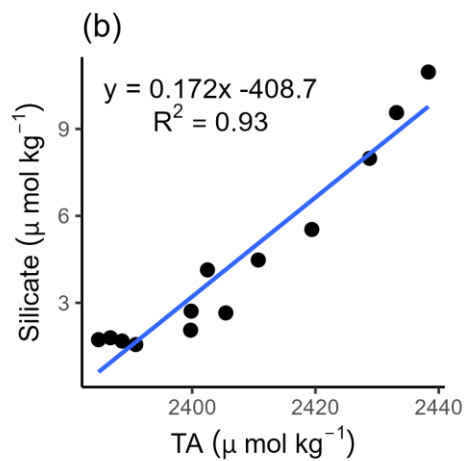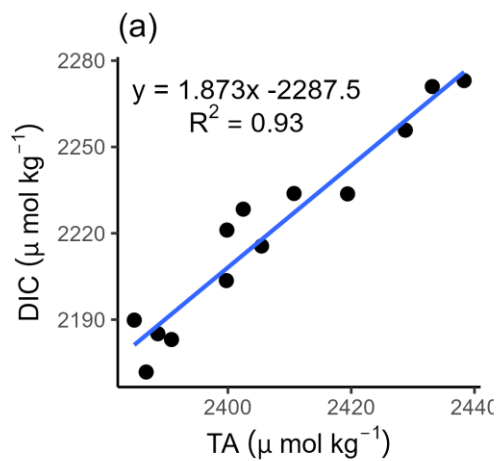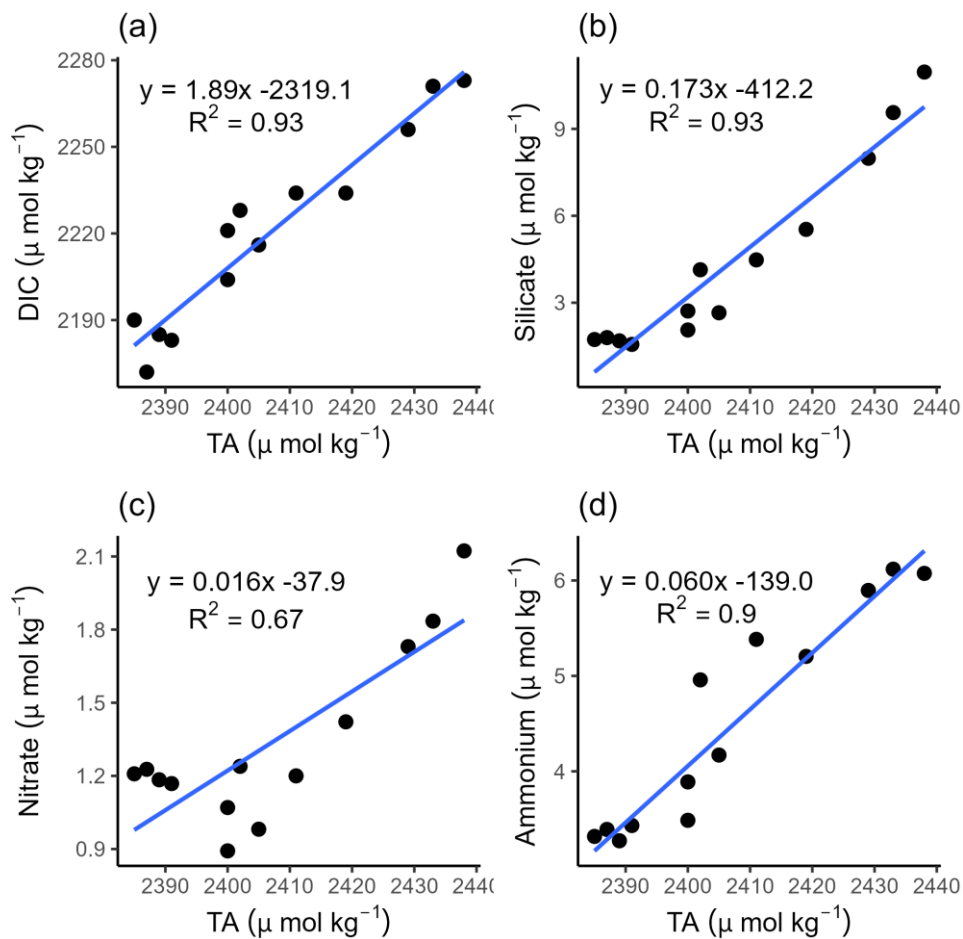
Figure 5 Correlations of TA with a) dissolved inorganic carbon (DIC), b) silicate, c) nitrate, and d) ammonium during ebb tide in the Ameland Inlet.

4 Discussion

4.1 Spatial TA variability

Hoppema (1990) reported TA distributions in the westernmost part of the Dutch Wadden Sea around the barrier islands Texel, Vlieland, and Terschelling. He focused on the tidal basins drained by the tidal inlets Marsdiep and Vlie located more to the west than our sampling stations (not visible on the map). Hoppema (1990) did not observe a~~n~~ continuous increase of salinity in the Wadden Sea from the fresh water source towards the North Sea ~~ocean~~ and associated this to the influence of tidal differences and an arbitrary sampling scheme. The presence (dominance) of North Sea ~~sea~~water in the Dutch Wadden Sea and on the tidal flats is supported by our transect data, which show relatively high salinities at coastal North Sea level. Brackish salinities were only detected in the large Ems-Dollard Inlet ~~Estuary~~, which receives ~~high discharges of~~ fresh water from the river Ems, and ~~also~~ close to Harlingen and Lauwersoog, which have direct fresh water inflows by smaller rivers and streams. The absence of clear salinity gradients in the more eastern ~~this~~ part of the Dutch Wadden Sea investigated in our study suggest that most of the IJsselmeer discharge was exchanged with the North Sea through the Marsdiep (e.g., Duran-Matute et al., 2014).

The spatial TA data by Hoppema (1990), show lower TA concentrations at stations with more fresh water influence and higher TA concentrations in the tidal inlets. The data of this study also show high TA concentrations in the tidal inlets, suggesting TA generation in sediments, which is possibly fueled by high imports of nutrients and OM (van Beusekom and De Jonge, 2002). The even higher TA concentrations at stations with lower salinities close to the mainland observed in this study also show the influence from the catchment area on the coast, and possibly TA generation in the shallow sediments near the coast. In May (1986), Hoppema~~'s~~ (1990) found ~~data showed~~ TA concentrations ranging between 2319 and 2444 µmol TA kg^{-1} ~~TA~~ at salinities between 18.62 and 29.17. Our~~, while our~~ lowest observed TA concentration was 2332 µmol TA kg^{-1} ~~TA~~ at a salinity of 32.14, and our highest TA concentration was 2517 µmol TA kg^{-1} ~~TA~~ at a salinity of 20.25 close to the coastal mainland. A ~~C~~comparison~~ng~~ of both studies~~, one can say~~ shows that the general TA level~~s~~ ~~of TA was~~ are in a similar range, but that the spatial gradients are opposite.

A conservative mixing between TA and salinity is only visible in the Ems-Dollard Inlet and the Vlie Inlet (Fig. 3). While the conservative mixing in the Ems-Dollard Inlet is more dominated by the fresh water discharge from the Ems River, t~~T~~he conservative mixing in the Vlie Inlet is more dominated by North Sea water passing through this deep inlet and allowing more North Sea water to be transported towards the coast. ~~can be explained by the fact that more North Sea water pass through the deeper inlets and transport more seawater towards the coast.~~ ~~After the Marsdiep Inlet, the~~ The Vlie Inlet has the highest average tidal prism and is the second largest inlet ~~after the Marsdiep Inlet~~ in the Dutch Wadden Sea (Elias et al., 2012). Similar to our findings, Hoppema (1990) noted a linear mixing of TA and salinity in the Vlie Inlet, and suspected a lower fresh water contribution there as well, which is in accordance with model data (Duran-Matute et al., 2014).

315 In the Ems-Dollard Inlet, conservative mixing was observed, indicating minor contributions from other sources. In a previous
316 study, Norbisrath et al. (2023) observed very high TA concentrations and TA generation in the upper tidal river of the highly
317 turbid Ems Estuary, which may explain the high levels of TA in the Ems-Dollard Inlet~~estuary~~ (at low salinities) observed in
318 this study.

319 Hoppema (1990) also observed a range of ~~identified varying~~ TA concentrations within the Dutch Wadden Sea and related
320 these to different sinks and sources. TA sinks can be calcium carbonate ($CaCO_3$) precipitation, or extraction of seawater
321 carbonate by mollusks (e.g., Chen and Wang, 1999;Hoppema, 1990). Variable fresh_water inflows can either serve as a sink
322 or a source (e.g., Chen and Wang, 1999;Hoppema, 1990). Other TA sources can be $CaCO_3$ dissolution, anaerobic metabolic
323 processes in the sediment, or erosion of TA enhancing sediments (e.g., Hoppema, 1990;Chen and Wang, 1999).

324 ~~Since we observed~~Except for the Ems-Dollard Inlet and close to Harlingen, we observed mainly ~~constant~~ marine salinities (>
325 30)~~, but~~ and higher TA values in the Dutch Wadden Sea than in the North Sea. ~~, w~~We therefore exclude possible TA sinks and
326 focus only on TA sources. According to Hoppema (1990), the main causes for TA variations in the Dutch Wadden Sea were
327 fresh_water inflows and sources in the sediment. In our study, fresh_water inflows with high TA concentrations were only
328 observed in the ~~Ems Estuary and~~ Ems-Dollard Inlet, but not around the islands and the tidal flats. For a further TA source
329 identification in the Dutch Wadden Sea, we investigated the TA variability during ebb tide in a tidal channel ~~a tidal cycle~~
330 close to Ameland.

4.2 Determination of TA generation

332 Burt et al. (2016) and Schwichtenberg et al. (2020) indicated ~~assumed~~ TA generation in the Wadden Sea as an important source
333 for the North Sea's carbon storage capacity. Here, we want to further identify TA generation and potential TA sources.
334 In a study from the late 1980s ~~early 1990s~~, Hoppema (1993) observed a tidal cycle in the Marsdiep in May and September.
335 Focusing on TA, DIC, and oxygen, he also observed increasing TA values during ebb tide and assumed the tidal flats and
336 discharging rivers and canals as TA sources. Comparing our present TA data and the historical TA data, there is not a large
337 difference in the range of values observed during a tidal cycle.~~Our present TA data and the historical TA data show no large~~
338 ~~differences in the range of values observed during a tidal cycle.~~ However, a further ~~in~~-depth interpretation and comparison
339 of both TA data sets is limited by the low number of data,~~would exceed the capacity of these data,~~ leading us to focus on TA
340 generation during our cruise.
341 ~~Our observation of a TA generation of 7.6 µmol kg^{-1} h^{-1} TA during ebb tide supports the assumption of the Wadden Sea being~~
342 ~~a TA source for the North Sea. With the tidal prism of the Ameland Inlet estimated by Louters and Gerritsen (1994), we~~
343 ~~estimated an upper bound TA export from the Dutch Wadden Sea into the North Sea on the order of 23.9 mol TA during ebb~~
344 ~~tide (3.5 mol h^{-1} TA) between spring and summer. This TA export is a rough maximum estimate, because some waters in the~~
345 ~~main tide channels have no direct contact to the areas of the tidal flats.~~ We made a very rough first estimate of the daily TA
346 export. By using a 3D ecosystem model, Schwichtenberg et al. (2020) estimated ~~assumed~~ an annual export of 10 to 14 Gmol
347 TA yr^{-1} ~~TA~~ for the entire Dutch Wadden Sea. Given that the Borndiep tidal basin covers about 14% of the Dutch Wadden Sea

348 and assuming no seasonal dynamics, our estimate of 12.7 Mmol d^{-1} compares well with the annual averaged model estimate
349 of 4.6 Mmol TA d^{-1}, but the overestimation suggests that seasonal dynamics may be involved. ~~However,~~ Since our TA export
350 based only on a half tidal observation, the~~an~~ inclusion of it ~~our TA export~~ into the model used by Schwichtenberg et al. (2020)
351 would be unreliable ~~, since our TA export based only on one tidal observation~~ (personal communication J. Pätsch, 2022). To
352 test whether the observed TA generation matches their suggested TA export, ~~more~~ observational data of at least each season
353 are required. ~~We suggest at least seasonal observational data in order~~ to run the model and gain a representative result (personal
354 communication J. Pätsch, 2022). ~~as future work.~~

4.3 TA source attribution

4.3.1 Local sediment outwash

357 In order to gain further insight into potential sources of TA, we compared our TA and nutrient data. ~~included nutrients in our~~
358 ~~investigation.~~ The main focus was on dissolved silicate (Si) as van Bennekom et al. (1974) showed that this nutrient is depleted
359 in the Wadden Sea during the spring diatom blooms and further showed that pore water is the main source of dissolved Si
360 during summer. It is important to note that winter concentrations in the Rhine (main contributor to the IJsselmeer) have not
361 changed much since the 1970s and showing maximum concentrations of about 125 µmol Si L^{-1} in winter and clear seasonal
362 dynamics due to uptake by diatoms (unpublished results based on data provided by Pätsch (2024); available through
363 https://wiki.cen.uni-hamburg.de/ifm/ECOHAM/DATA_RIVER). ~~silicate that we used as a natural tracer since it is not directly~~
364 ~~provided anthropogenically and allowed us to determine the silicate source (van der Zee and Chou, 2005). van Bennekom et~~
365 ~~al. (1974)~~We identified a silicate increase of 1.4 µmol Si L^{-1} h^{-1} ~~Si~~ during ebb tide. ~~Silicate originates from dissolution of~~
366 ~~diatoms and pore water exchange in the Wadden Sea (van Bennekom et al., 1974;van der Zee and Chou, 2005). Here, we relate~~
367 ~~the silicate increase to pore water exchange, because it markedly increased during ebb tide. This assumption is supported by~~
368 ~~van Bennekom et al. (1974), who suggested silicate diffusion from interstitial water in the sediment as potential source, since~~
369 ~~very high silicate concentrations were found in deeper sediment layers (Rutgers van der Loeff, 1974).~~ Due to the absence of
370 large estuaries nearby and salinity consistently being above 32 at our tidal sampling station around the island of Ameland, we
371 exclude fresh water runoff as a major silicate source. ~~This can be supported by the relation between silicate and salinity in~~
372 ~~which we observed a non-conservative behavior (Table B1) and indicate~~. ~~Since TA behaves also non-conservative relative to~~
373 ~~salinity (Table B1), the silicate observations support the occurrence of~~ TA source~~ss in the tidal flats of~~ within the Wadden
374 Sea.
375 Submarine groundwater discharge (SGD) was identified as a source for nutrient fluxes in tidal flat ecosystems in previous
376 studies (e.g., Billerbeck et al., 2006;Røy et al., 2008;Santos et al., 2021;Waska and Kim, 2011;Wu et al., 2013). ~~Waska and~~
377 ~~Kim (2011) identified strong SGD contributing up to 50 to 70 % of the nutrient fluxes that fuel primary production in a tidal~~
378 ~~embayment (Hampyeong Bay) in southwest Korea. In May, they observed low salinities indicating freshwater. However, in~~
379 ~~September they observed constant marine salinities referring them to be exclusively composed of recirculating seawater.~~ Since

380 we ~~constantly~~ observed relatively constant marine salinities, we suspect that deep pore water flow (e.g., Røy et al.,
381 2008)~~recirculating marine groundwater~~ enriched with nutrients act as a source for our observed increasing TA and nutrients
382 parameters. TA generation in tidal flats was also observed by Faber et al. (2014), who focused on a large macro tidal
383 embayment in southern Australia. They also found increasing TA values during ebb tide, associated the TA increase with a
384 higher fraction of pore water, and determined the tidal cycle as the controlling force for pore water exchange. Their findings
385 and the observed silicate outwash support our assumption that TA is generated in the sediments of the tidal flats and is washed
386 out during ebb tide. In addition, we exclude lateral advected signals from more western regions as the Vlie Inlet, since the TA
387 concentrations in the surface transect samples in the Vlie Inlet (except of the two samples close to the coastal mainland near
388 Harlingen) were in the same range as the other observed TA concentrations and were smaller than ~~below~~ the increasing TA
389 concentrations during ebb tide. Both increases in TA and silicate are ~~clearly~~ tidal signals, and we ~~clearly~~ identify TA generation
390 in the sediments of the tidal flats here as the major local TA source~~s~~.

4.3.2 TA generating processes

392 The observed TA generation of 7.6 µmol TA kg^{-1} h^{-1} ~~TA~~ and the silicate increase of 1.4 µmol Si L^{-1} h^{-1} ~~Si~~ indicated an excess
393 of TA (also Fig. 5b). A given ~~a~~ TA:silicate ratio of 2:1 (Marx et al. 2017)~~, and under the condition of silicate being bound in~~
394 ~~minerals, which~~ would ~~then~~ account for a TA generation of 2.8 µmol TA kg^{-1} h^{-1} ~~TA. However, when silicate occurred~~
395 ~~dissolved in water it does not contribute to TA generation (Meister et al., 2022). A TA excess related to silicate was also~~
396 ~~observed in the correlation between TA and silicate (Fig. 5b).~~ High Si concentrations in tidal flat pore water (Rutgers van der
397 Loeff, 1974) and in situ production of Si from dissolving diatom frustules are the most probable sources of the Si (e.g., van
398 Bennekom et al., 1974). Since we observed more TA generated than silicate being washed out, other biogeochemical processes
399 must be responsible for the TA generation in the sediments of the tidal flats in the Dutch Wadden Sea.
400
401 ~~We~~ With the observed omega values, we ~~exclude~~ exclude CaCO$_3$ dissolution as TA source in the overlying water, since the Ω ~~omega~~
402 values were clearly supersaturated with $\Omega > 1$(Fig. 4h,i~~f~~, Table B1). The continuous calcite supersaturation nicely indicated
403 the inflow and dominance of North Sea water during the flood, with Ω ~~omega~~ values similar to previously observed North Sea
404 values ($\Omega \sim 3.5$ to 4) (Charalampopoulou et al., 2011;Carter et al., 2014). ~~However, because of the Ω supersaturation of the~~
405 ~~overlying water and a lack of pore water data, we were unable to determine if TA generation by CaCO$_3$ dissolution occurs in~~
406 ~~deeper sediment layers. There,~~ In pore water, carbonate undersaturation and associated CaCO$_3$ dissolution can only be driven
407 metabolically, due to, ~~when~~ CO$_2$ ~~is~~ produc~~tion by~~ ~~ed during~~ OM remineralization, or due to the reoxidation of compounds
408 reduced previously by anaerobic processes ~~when reduced compounds that were previously produced during anaerobic~~
409 ~~processes are oxidized and lead to undersaturation with respect to carbonates~~ (Brenner et al., 2016;Jahnke et al., 1994).
410 Other potential sources of TA generation in the sediments can be further narrowed down by a more detailed interpretation of
411 changes both in DIC (ΔDIC) and TA (ΔTA) during ebb tide, and their combination with various nutrient ratios.

412 ~~A more detailed interpretation of ΔDIC, ΔTA, and various nutrient ratios, further narrows down the potential sources of TA~~
413 ~~generation in the sediments and used an upper bound estimate for CaCO₃ dissolution.~~ The correlation of DIC and TA reveals
414 an excess of released DIC compared to TA (Fig. 5a), as indicated by the slope of 1.87, while we observed an increase in DIC
415 (ΔDIC) almost twice as high as in TA (ΔTA). The high ΔDIC points to high aerobic OM degradation and remineralization,
416 resulting in high CO_2 productionexport. High aerobic OM degradation was also previously observed in the heterotrophic
417 Wadden Sea (e.g., De Beer et al., 2005;van Beusekom et al., 1999), assuming an OM degradation and remineralization
418 occurring in the water and sediment in about equal parts (van Beusekom et al., 1999). High OM degradation is ~~also~~ indicated
419 by the increasing C_{org}:N ratios of SPM during ebb tide (Fig. 4kh, Table B1). Because we observed constant coastal North Sea
420 salinities, we rule out fresh water runoff and terrestrial signals as source for the increasing C_{org}:N ratios of SPM. We assume
421 that fresh OM is rapidly degraded in the water column, and the older OM settles on and in the sediment where the degradation
422 continuoeus and where it is resuspended at the low prevailing water levels during ebb ~~by the water exchange with outflowing~~
423 ~~water~~. Therefore, we assume that the increase of SPM concentrations and their C_{org}:N ratios is an indicator for older and more
424 refractory OM. The increase in TA concentrations point to anaerobic processes, $CaCO_3$ dissolution, or a combination thereof
425 as TA sources occurring in the sediments.
426
427 For ~~the~~ an upper bound estimate of sedimentary $CaCO_3$ dissolution as source of TA, we considered a DIC:TA ratio of 1:2. ~~,~~
428 ~~we assumed CaCO₃ dissolution in the sediments with the DIC:TA ratio of 1:2 as source of TA.~~ Considering this ratio and the
429 observed ΔTA of 51.6 µmol TA kg⁻¹ ~~TA~~, $CaCO_3$ dissolution would lead to a potential ΔDIC of 25.8 µmol DIC kg⁻¹. ~~DIC of~~
430 ~~the observed ΔTA would be produced by CaCO₃ dissolution.~~ The remaining potential 75.5 µmol DIC kg⁻¹ ~~DIC~~ (101.3 – 25.8
431 µmol DIC kg⁻¹ ~~DIC~~) of the observed (ΔDIC) could then be produced by OM degradation and remineralization, and would,
432 using the expected Redfield ratio of C:N (6.6), correspond to an estimated potential dissolved inorganic nitrogen (DIN)
433 production of 11.4 µmol DIN kg⁻¹ ~~DIN~~. However, this estimated potential DIN production (11.4 µmol DIN kg⁻¹ ~~DIN~~) of OM
434 degradation and remineralization exceedsed the observed increase of ΔDIN (3.97 µmol DIN L⁻¹ ~~DIN~~; Table B1, sum of NO_3^-
435 , NO_2^- and NH_4^+) during ebb tide. Based on ~~With~~ this estimation and the assumption that all DIN produced is released and thus
436 lost, TA is probably produced by $CaCO_3$ dissolution and anaerobic metabolic processes other than denitrification in the
437 sediment. In addition to that, and with a N-focused perspective, the DIN loss also hints to the occurrence of other processes
438 that consume nitrogen species but have no net effect on TA, such as anammox and coupled nitrification-denitrification (Hu
439 and Cai, 2011;Middelburg et al., 2020). The suggested DIN loss can be supported by considering the marine DIN:Si ratio,
440 which is supposed to be about 1:1 (Brzezinski, 1985). We observed DIN:Si ratios decreasing from 2.7 to 0.8 during ebb ~~from~~
441 ~~high tide to low~~ tide, showing that ~~. The decreasing ratios show that~~ both parameter concentrations increased ~~during ebb tide~~,
442 whereby DIN concentrations increased less ~~lower~~ than silicate concentrations. ~~We observed a~~ The silicate excess with respect
443 to DIN at the end of ebb tide, supportsing the DIN loss.
444 Denitrification, the anaerobic irreversible reduction of NO_3^- to N_2 that generates 0.9 mole TA by using 1 mole NO_3^- as electron
445 acceptor (Chen and Wang, 1999) is a net TA source. Denitrification depends on the supply of nitrate, which seasonally varies

Formatiert: Tiefgestellt

Formatiert: Tiefgestellt

Formatiert: Nicht Hochgestellt/ Tiefgestellt

446 (van der Zee and Chou, 2005 and references therein). Generally, nitrate is depleted in summer due to high photosynthetic
447 activity turnover rates and occurs in higher concentrations in winter (Kieskamp et al., 1991;Jensen et al., 1996;van der Zee and
448 Chou, 2005). This seasonality lead to denitrification rates also being lower in summer and higher in winter (Kieskamp et al.,
449 1991;Jensen et al., 1996). In previous studies, Faber et al. (2014) identified denitrification as a minor source of TA due to low
450 denitrification rates, and also Kieskamp et al. (1991) observed low denitrification rates in the Wadden Sea, with low nitrate
451 concentrations (< 2.5 µmol L^{-1}) in the overlying water. We observed nitrate concentrations (< 2.17 µmol L^{-1}) lower than the
452 concentration sufficient for denitrification assumed by Kieskamp et al. (1991). Therefore, we do not exclude denitrification,
453 but suspect it as a minor source of TA in the Dutch Wadden Sea at least in spring and summer due to the seasonal lack of
454 nitrate. Thomas et al. (2009) detected TA seasonality in the southern bight of the North Sea, which is also influenced by the
455 TA generation in the Wadden Sea. We support their findings of lowered TA generation by denitrification in late spring and
456 early summer. In addition, the calculated potential DIN excess compared to the observed DIN not only hints to other N
457 consuming processes that have no effect on TA, but also suggests that allochthonous nitrate would be needed to fuel the TA
458 increase by denitrification. In addition, the albeit low availability of nitrate indicates to predominantly aerobic metabolic
459 activity during the time of our observations, which is in line with earlier studies reporting an enhanced relevance of anaerobic
460 activity later in summer (Luff and Moll, 2004;Thomas et al., 2009).

461

462 The simultaneous increase of ammonium and TA (Fig. 4c, 4d, 5d) is important to notice, because under oxic conditions the
463 occurrence of ammonium is coupled with nitrification, a process that consumes ammonium and also TA (Chen and Wang,
464 1999).
465 However, under anoxic conditions, such as in deeper sediment layers, ammonium cannot be reoxidized, accumulates and is
466 washed out during ebb tide. Since we observed low nitrate concentrations and rule out terrestrial nitrate inputs here, the increase
467 in ammonium and TA implies the occurrence of other anaerobic processes of the redox system, such as sulfate and iron
468 reduction, to generate TA in the deeper, anoxic sediment layers in the Dutch Wadden Sea.
469 Another source of TA in sediments is aerobic OM respiration with the associated formation of ammonium while consuming
470 H$^+$ (Blackburn and Henriksen, 1983;Berner et al., 1970;Brenner et al., 2016). The observed increasing ammonium
471 concentrations (Fig. 4c) could be associated with aerobic OM degradation leading to ammonium formation. The resulting
472 ammonium formation in the upper oxygenated sediment layers would increase DIC by the production of CO$_2$, and increase
473 TA by the consumption of H$^+$ (Fig.5) (Brenner et al., 2016). In sediments, the production of one mole ammonium (from
474 ammonia) would then generate one mole TA (Berner et al., 1970;Meister et al., 2022). In contrast, in the water column, the
475 aerobic respiration of OM produce CO$_2$ and increase DIC, also visible in decreasing pH values (Fig. 4g), but consume TA and
476 would not produce ammonium (Chen and Wang, 1999). Therefore, aerobic OM respiration in the water column could only
477 explain the higher increase in DIC than in TA, but not the simultaneous increase in TA and ammonium (Fig. 5). Based on this,
478 we assume that OM respiration associated with TA generation occurs in the sediments, leading to TA and DIC generation and
479 also to ammonium production, being washed out during ebb tide. The produced ammonium is then also accessible for

480 ~~nitrification that produces nitrate. A slightly increased nitrate concentration in the most upper sediment layers was observed~~
481 ~~by Beck et al. (2008a) in the German Wadden Sea. This observation, a potential nitrate reservoir, nitrate production due to OM~~
482 ~~degradation and nitrification occurring in the upper oxygenated sediment layers (Martin and Sayles, 1996), or a combination~~
483 ~~thereof could explain the observed low increasing nitrate concentrations during ebb tide. However, as we rule out terrestrial~~
484 ~~nitrate imports as nitrate source here, the simultaneous increase of TA and nitrate is noticeable for us, because nitrification~~
485 ~~consumes TA (Brenner et al., 2016). We assume that potential nitrification has a minor effect on TA, since we observed only~~
486 ~~low nitrate concentrations and a really low increase of nitrate compared to the increase of ammonium and TA during ebb tide.~~
487 ~~Low nitrate concentrations resulting in a reduced availability of bound oxygen, i.e., electron acceptors. This promotes the~~
488 ~~occurrence of other anaerobic processes of the redox system to generate TA in the deeper, anoxic sediment layers in the Dutch~~
489 ~~Wadden Sea, such as sulfate and iron reduction.~~

490 Sulfate reduction followed by iron reduction and the formation and burial of pyrite are net sources of TA, since TA
491 consumption by reoxidation is excluded when buried in sediments (Berner et al., 1970;Faber et al., 2014). Whether these
492 processes contribute to TA generation in the deeper sediments of the Dutch Wadden Sea cannot be further identified without
493 the necessary data. However, sulfate reduction was also mentioned as source of TA by Thomas et al. (2009). The temporary
494 slight appearance of noticeable sulfuric odor could be another indirect indicator for the occurrence of sulfate reduction. In
495 previous studies of tidal flats in the German Wadden Sea, Beck et al. (2008a);(2008b) observed increasing TA concentrations
496 with depth and identified sulfate reduction as the most important process for anaerobic OM remineralization in pore water
497 cores. ~~Sulfate reduction releases 1.14 mole TA with the oxidation of one mole carbon of POC , and iron reduction releases~~
498 ~~8.14 mole TA with the oxidation of one mole carbon of POC, indicating that both processes are large sources of TA generation~~
499 ~~(Brenner et al., 2016), but further studies are needed to support this.~~

500

501 A strict comparison of the northern and the western parts of the Wadden Sea is difficult because the areas vary in terms of OM
502 import and eutrophication effects (van Beusekom et al., 2019), sediment composition, and extent between the barrier islands
503 and the mainland, all of which influence the occurrence and interaction of biogeochemical processes (Schwichtenberg et al.,
504 2020). The area characteristics of the northern and western Wadden Sea differ especially in terms of OM turnover being lower
505 in the norther Wadden Sea. A previous study by Brasse et al. (1999) identified high TA and DIC concentrations in the sediment
506 of the North Frisian Wadden Sea and identified $CaCO_3$ dissolution and sulfate reduction as major TA sources, which is
507 consistent with our findings.

508 **5 Conclusion**

509 The Dutch Wadden Sea is a unique and highly dynamic ecosystem. ~~While observing the spatial TA distribution and TA~~
510 ~~generation in the Dutch Wadden Sea, w~~We observed ~~detected~~ higher TA values in the Dutch Wadden Sea than in the North
511 Sea and identified the Dutch Wadden Sea ~~clearly~~ as a TA source for the North Sea's carbonate system. Compared to previous

512 studies (Hoppema, 1990, 1993), the TA values we observed were in a similar range, with high TA values in the tidal basins.

513 Beside the need for seasonal observations, future work should also focus on ~~the tidal end-members to better understand the~~

514 ~~general~~ regional and seasonal impacts ~~influence~~ of fresh_water inflows ~~of TA~~ on the TA status in the Dutch Wadden Sea.

515 By observing salinity and using dissolved silicate as a tracer, we excluded fresh_water ~~dilution~~ and river runoff as significant

516 TA sources on the tidal flats, and instead, deduced ~~identified~~ local outwash from the sediments as sources of TA. Considering

517 various stoichiometries, we suggest that a~~A~~erobic~~, metabolic processes such as~~ $CaCO_3$ dissolution ~~and ammonium formation~~

518 ~~seem to dominate~~ generates TA ~~generation~~ in the upper oxic sediment layers ~~and the overlying water~~, and ~~while~~ anaerobic,

519 metabolic processes such as denitrification, sulfate and iron reduction are potential TA sources in the deeper anoxic sediment

520 layers. However, in spring and early summer, denitrification seems to play a minor role in generating TA in the sediments of

521 the Dutch Wadden Sea due to seasonality and associated limited nitrate availability.

522 **6 Appendices**

523 **Appendix A**
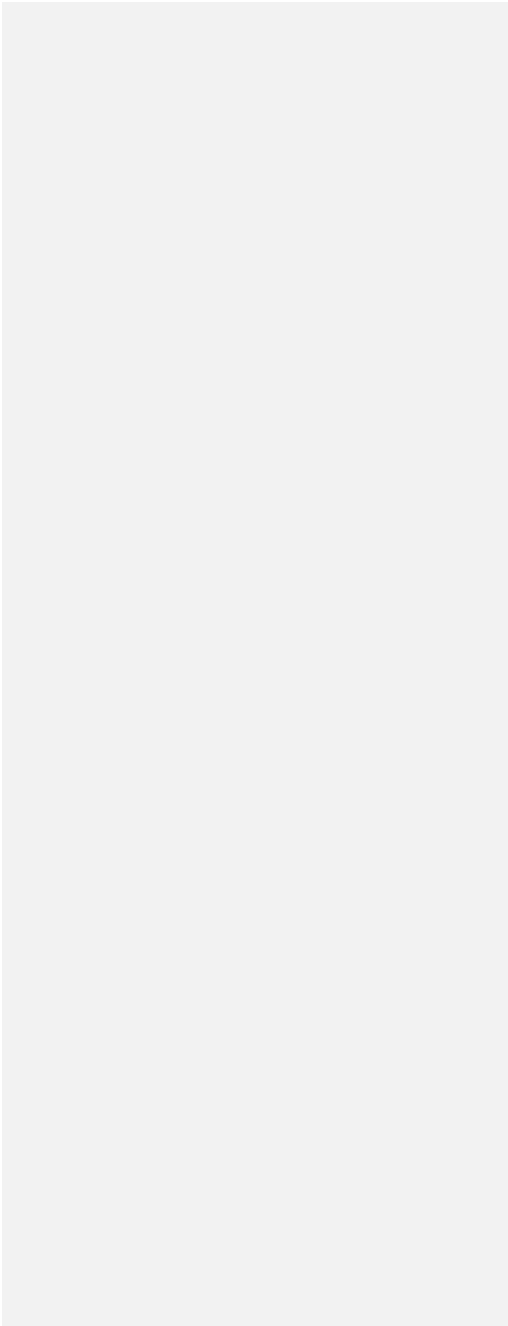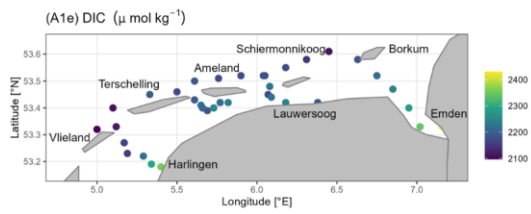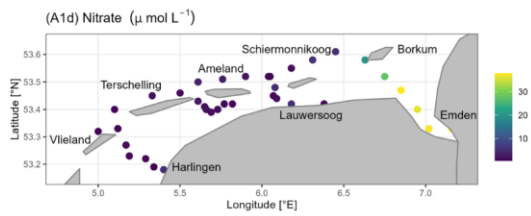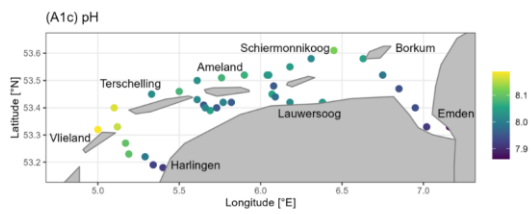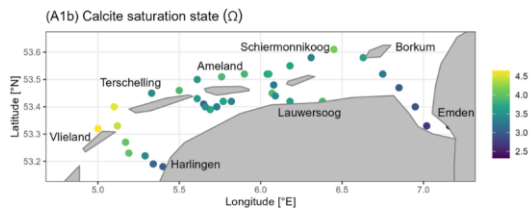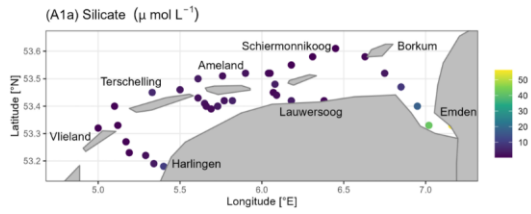
525 **Figure A1** ~~Spatial distribution~~ ~~Latitudinal and longitudinal distribution~~ of A1a) silicate (Si; μmol L^{-1}), A1b) calcite saturation
526 state (Ω), A1c) pH, A1d) nitrate (NO$_3^-$; μmol L^{-1}), and A1e) dissolved inorganic carbon (DIC; μmol kg^{-1}) from surface water
527 samples in May 2019.
528

529 **Appendix B**

530 **Table B1** Half Ttidal cycle sample parameter during ebb tide. Sample no. 545 is the first sample at high tide and sample no.
531 557 is the last sample at ebb low tide on 21 May 21ˢᵗ 2019 (53.38°N & 5.62°E). Shown are rounded up values of temperature
532 (Temp), salinity (Sal), total alkalinity (TA), dissolved inorganic carbon (DIC), silicate (Si), nitrate (NO_3^-), nitrite (NO_2^-),
533 ammonium (NH_4^+), dissolved inorganic nitrogen (DIN), the amount of carbon (C) and organic carbon (C_{org}) of SPM, the
534 amount of nitrogen (N) of SPM, the calcite (Ca) and aragonite (Ar) saturation states, the pH, and phosphate (PO_4^{3-}) per sample.

Sample No.	Time [UTC]	Temp [°C]	Sal	TA [μmol kg⁻¹]	DIC [μmol kg⁻¹]	Si [μmol L⁻¹]	NO_3^- [μmol L⁻¹]	NO_2^- [μmol L⁻¹]	NH_4^+ [μmol L⁻¹]
545	10:46	13.26	32.52	2387	2172	1.84	1.26	0.19	3.47
546	11:19	13.25	32.52	2385	2190	1.77	1.24	0.19	3.40
547	11:49	13.28	32.52	2389	2185	1.72	1.21	0.19	3.35
548	12:23	13.38	32.52	2391	2183	1.6	1.19	0.19	3.52
549	13:35	14.32	32.50	2400	2204	2.11	0.91	0.25	3.57
550	14:05	14.61	32.50	2400	2221	2.78	1.09	0.29	3.98
551	14:36	14.64	32.51	2405	2216	2.72	1.01	0.29	4.27
552	15:26	14.73	32.51	2411	2234	4.59	1.23	0.34	5.51
553	15:42	14.77	32.51	2402	2228	4.24	1.26	0.33	5.08
554	16:04	14.72	32.51	2419	2234	5.66	1.46	0.36	5.33
555	16:38	14.66	32.51	2428	2256	8.18	1.77	0.43	6.04
556	17:07	14.68	32.51	2433	2271	9.79	1.87	0.47	6.27
557	17:32	14.70	32.50	2438	2273	11.22	2.17	0.50	6.22

Sample No.	Time [UTC]	DIN [μmol L⁻¹]	C / C_{org} (SPM) [μmol L⁻¹]	N (SPM) [μmol L⁻¹]	C_{org}:N (SPM)	SPM [mg L⁻¹]	Ca / Ar [Ω]	pH	PO_4^{3-} [μmol L⁻¹]
545	10:46	4.93	86.8 / 65.1	8.8	7.4	12.8	3.8 / 2.4	8.07	0.12
546	11:19	4.83	72.7 / 42.4	7.4	5.8	8.7	3.5 / 2.3	8.03	0.11
547	11:49	4.76	112.4 / 93.4	9.6	9.7	15.4	3.7 / 2.3	8.05	0.11
548	12:23	4.91	108.5 / 104.6	9.9	10.5	16.8	3.7 / 2.4	8.05	0.12
549	13:35	4.73	111.1 / 97.8	8.8	11.1	13.9	3.6 / 2.3	8.01	0.32
550	14:05	5.37	233.0 / 180.3	17.7	10.2	32.2	3.3 / 2.1	7.97	0.42
551	14:36	5.56	193.2 / 174.3	14.5	12.0	29.6	3.5 / 2.2	7.99	0.47
552	15:26	7.08	248.6 / 163.5	18.4	8.9	34.3	3.3 / 2.1	7.96	0.57
553	15:42	6.67	257.6 / 199.3	18.3	10.9	41.6	3.2 / 2.1	7.95	0.54
554	16:04	7.15	324.4 / 271.1	23.2	11.7	55.0	3.4 / 2.2	7.98	0.54
555	16:38	8.24	440.4 / 345.2	29.2	11.8	75.7	3.2 / 2.1	7.95	0.58
556	17:07	8.61	430.5 / 363.3	27.9	13.0	82.4	3.1 / 2.0	7.93.	0.62
557	17:32	8.90	308.9 / 199.1	21.2	9.4	48.8	3.1 / 2.0	7.93	0.63

Formatierte Tabelle

535 **Table B2** Half tidal cycle sample parameter during high tide. Sample no. 564 is the first sample at low tide and sample no.
536 578 is the last sample at high tide on 23 May 2019 (53.39°N & 5.63°E, 5.62°E*). Shown are rounded up values of temperature
537 (Temp), salinity (Sal), total alkalinity (TA), dissolved inorganic carbon (DIC), silicate (Si), nitrate (NO$_3^-$), nitrite (NO$_2^-$),
538 ammonium (NH$_4^+$), dissolved inorganic nitrogen (DIN), the amount of carbon (C) and organic carbon (C$_{org}$) of SPM, the
539 amount of nitrogen (N) of SPM, the calcite (Ca) and aragonite (Ar) saturation states, the pH, and phosphate (PO$_4^{3-}$) per sample.

Sample No.	Time [UTC]	Temp [°C]	Sal	TA [µmol kg^{-1}]	DIC [µmol kg^{-1}]	Si [µmol L^{-1}]	NO$_3^-$ [µmol L^{-1}]	NO$_2^-$ [µmol L^{-1}]	NH$_4^+$ [µmol L^{-1}]
564	05:09	14.04	32.7	2431	2246	8.53	1.25	0.47	3.31
565	05:32	14.02	32.7	2441	2287	9.14	1.26	0.45	3.08
566	06:01	13.95	32.7	2436	2284	8.88	1.33	0.38	2.46
567	06:33	14.16	32.7	2443	2284	8.68	0.95	0.37	2.37
568	07:02	14.21	32.7	2432	2280	6.94	0.75	0.34	2.63
569	07:31	14.15	32.6	2401	2223	2.12	0.98	0.27	4.12
570	08:04	14.20	32.6	2403	2218	2.10	1.04	0.27	3.88
571	08:35	14.27	32.6	2409	2228	2.15	0.92	0.25	4.18
572	09:04	14.37	32.5	2400	2209	1.88	1.00	0.22	3.86
573	09:34	14.16	32.5	2398	2200	1.70	1.03	0.21	3.51
574*	10:02	14.17	32.5	2391	2197	1.72	1.07	0.21	3.40
575*	10:34	14.11	32.5	2389	2195	1.78	1.18	0.20	3.45
576	11:04	14.21	32.5	2390	2187	1.76	1.12	0.19	3.29
577	11:34	14.50	32.5	2399	2193	1.66	1.10	0.20	3.32
578	12:03	13.96	32.5	2390	2187	1.75	1.41	0.19	3.72

Sample No.	Time [UTC]	DIN [µmol L^{-1}]	C / C$_{org}$ (SPM) [µmol L^{-1}]	N (SPM) [µmol L^{-1}]	C$_{org}$:N (SPM)	SPM [mg L^{-1}]	Ca / Ar [Ω]	pH	PO$_4^{3-}$ [µmol L^{-1}]
564	05:09	5.03	353.7 / 253.2	27.5	9.2	52.3	3.04 / 2.2	7.99	0.38
565	05:32	4.78	333.5 / 220.1	26.1	8.4	49.7	3.0 / 1.9	7.92	0.37
566	06:01	4.17	330.3 / 232.9	25.5	9.1	51.7	2.9 / 1.9	7.91	0.34
567	06:33	3.68	274.7 / 195.7	21.8	9.0	36.9	3.0 / 1.9	7.92	0.33
568	07:02	3.72	317.8 / 220.2	24.5	9.0	46.1	2.9 / 1.9	7.91	0.32
569	07:31	5.37	88.6 / 59.1	7.0	8.5	14.7	3.3 / 2.1	7.98	0.33
570	08:04	5.20	96.8 / 73.6	8.8	8.4	18.1	3.4 / 2.2	7.99	0.30
571	08:35	5.35	114.2 / 109.6	9.9	11.0	14.8	3.3 / 2.1	7.98	0.32
572	09:04	5.08	107.5 / 73.9	9.9	7.5	16.4	3.5 / 2.2	8.00	0.26
573	09:34	4.75	82.1 / 72.7	7.2	10.0	11.8	3.6 / 2.3	8.02	0.21
574*	10:02	4.68	85.2 / 62.9	7.2	8.7	9.9	3.5 / 2.3	8.01	0.18
575*	10:34	4.83	83.5 / 65.9	7.2	9.2	11.1	3.5 / 2.3	8.01	0.16

576	11:04	4.60	82.7 / 52.1	8.2	6.3	8.5	3.7 / 2.3	8.03	0.14
577	11:34	4.62	65.8 / 50.8	6.5	7.8	7.2	3.7 / 2.4	8.03	0.16
578	12:03	5.32	71.6 / 54.6	7.7	7.1	7.7	3.7 / 2.3	8.04	0.11

Data availability

The data of this study are either presented in the article or are available upon request from the corresponding author.

Author Contributions

MN wrote the manuscript, did the carbon sampling and sample measurement, analyzed and evaluated the data, and led the study. JvB led the research cruise. JvB and HT contributed with editorial and scientific recommendations. MN prepared the manuscript with contribution from all co-authors.

Competing interests

The contact author has declared that none of the authors has any competing interests.

Acknowledgement

We thank the crew from RV *Ludwig Prandtl* for their support during the cruise. We thank Leon Schmidt for the nutrient sampling and measurements, and Marc Metzke for the C/N measurements. We further thank the Editor Xinping Hu and two anonymous reviewers for their constructive comments, which greatly improved this manuscript.

Financial support

This research has been funded by the German Academic Exchange Service (DAAD, project: MOPGA-GRI, grant no. 57429828), which received funds from the German Federal Ministry of Education and Research (BMBF).

References

Abril, G., and Frankignoulle, M.: Nitrogen–alkalinity interactions in the highly polluted Scheldt basin (Belgium), Water Research, 35, 844-850, https://doi.org/10.1016/S0043-1354(00)00310-9, 2001.

Beck, M., Dellwig, O., Holstein, J. M., Grunwald, M., Liebezeit, G., Schnetger, B., and Brumsack, H.-J.: Sulphate, dissolved organic carbon, nutrients and terminal metabolic products in deep pore waters of an intertidal flat, Biogeochemistry, 89, 221-238, https://doi.org/10.1007/s10533-008-9215-6, 2008a.

Beck, M., Dellwig, O., Liebezeit, G., Schnetger, B., and Brumsack, H.-J.: Spatial and seasonal variations of sulphate, dissolved organic carbon, and nutrients in deep pore waters of intertidal flat sediments, Estuarine, Coastal and Shelf Science, 79, 307-316, https://doi.org/10.1016/j.ecss.2008.04.007, 2008b.

Berner, R. A., Scott, M. R., and Thomlinson, C.: Carbonate alkalinity in the pore waters of anoxic marine sediments 1, Limnology and Oceanography, 15, 544-549, https://doi.org/10.4319/lo.1970.15.4.0544, 1970.

Berner, R. A., Lasaga, A. C., and Garrels, R. M.: Carbonate-silicate geochemical cycle and its effect on atmospheric carbon dioxide over the past 100 million years, Am. J. Sci.;(United States), 283, doi:10.2475/ajs.283.7.641., 1983.

Billerbeck, M., Werner, U., Polerecky, L., Walpersdorf, E., DeBeer, D., and Huettel, M.: Surficial and deep pore water circulation governs spatial and temporal scales of nutrient recycling in intertidal sand flat sediment, Marine Ecology Progress Series, 326, 61-76, 2006.

Blackburn, T., and Henriksen, K.: Nitrogen cycling in different types of sediments from Danish waters 1, Limnology and Oceanography, 28, 477-493, https://doi.org/10.4319/lo.1983.28.3.0477, 1983.

Borges, A. V., Delille, B., and Frankignoulle, M.: Budgeting sinks and sources of CO_2 in the coastal ocean: Diversity of ecosystems counts, Geophysical research letters, 32, doi.org/10.1029/2005GL023053, 2005.

Bozec, Y., Thomas, H., Elkalay, K., and de Baar, H. J.: The continental shelf pump for CO_2 in the North Sea—evidence from summer observation, Marine Chemistry, 93, 131-147, https://doi.org/10.1016/j.marchem.2004.07.006, 2005.

Brasse, S., Reimer, A., Seifert, R., and Michaelis, W.: The influence of intertidal mudflats on the dissolved inorganic carbon and total alkalinity distribution in the German Bight, southeastern North Sea, Journal of Sea Research, 42, 93-103, 1999.

Brenner, H., Braeckman, U., Le Guitton, M., and Meysman, F. J.: The impact of sedimentary alkalinity release on the water column CO_2 system in the North Sea, Biogeosciences, 13, 841-863, https://doi.org/10.5194/bg-13-841-2016, 2016.

Brewer, P. G., and Goldman, J. C.: Alkalinity changes generated by phytoplankton growth, Limnology and Oceanography, 21, 108-117, https://doi.org/10.4319/lo.1976.21.1.0108, 1976.

Brzezinski, M. A.: The Si: C: N ratio of marine diatoms: interspecific variability and the effect of some environmental variables, Journal of Phycology, 21, 347-357, https://doi.org/10.1111/j.0022-3646.1985.00347.x, 1985.

Burchard, H., Flöser, G., Staneva, J. V., Badewien, T. H., and Riethmüller, R.: Impact of density gradients on net sediment transport into the Wadden Sea, Journal of Physical Oceanography, 38, 566-587, 2008.

Burt, W., Thomas, H., Hagens, M., Pätsch, J., Clargo, N., Salt, L., Winde, V., and Böttcher, M.: Carbon sources in the North Sea evaluated by means of radium and stable carbon isotope tracers, Limnology and Oceanography, 61, 666-683, https://doi.org/10.1002/lno.10243, 2016.

Carter, B. R., Toggweiler, J., Key, R. M., and Sarmiento, J. L.: Processes determining the marine alkalinity and calcium carbonate saturation state distributions, Biogeosciences, 11, 7349-7362, https://doi.org/10.5194/bg-11-7349-2014, 2014.

Charalampopoulou, A., Poulton, A. J., Tyrrell, T., and Lucas, M. I.: Irradiance and pH affect coccolithophore community composition on a transect between the North Sea and the Arctic Ocean, Marine Ecology Progress Series, 431, 25-43, https://doi.org/10.3354/meps09140, 2011.

Chen, C. T. A., and Wang, S. L.: Carbon, alkalinity and nutrient budgets on the East China Sea continental shelf, Journal of Geophysical Research: Oceans, 104, 20675-20686, https://doi.org/10.1029/1999JC900055, 1999.

Crutzen, P.: Geology of mankind, Nature, 415, https://doi.org/10.1038/415023a, 2002.

De Beer, D., Wenzhöfer, F., Ferdelman, T. G., Boehme, S. E., Huettel, M., van Beusekom, J. E., Böttcher, M. E., Musat, N., and Dubilier, N.: Transport and mineralization rates in North Sea sandy intertidal sediments, Sylt-Rømø basin, Wadden Sea, Limnology and Oceanography, 50, 113-127, 2005.

De Jonge, V., Essink, K., and Boddeke, R.: The Dutch Wadden Sea: a changed ecosystem, Hydrobiologia, 265, 45-71, https://doi.org/10.1007/BF00007262, 1993.

Dickson, A., and Millero, F. J.: A comparison of the equilibrium constants for the dissociation of carbonic acid in seawater media, Deep Sea Research Part A. Oceanographic Research Papers, 34, 1733-1743, https://doi.org/10.1016/0198-0149(87)90021-5, 1987.

Dickson, A. G.: An exact definition of total alkalinity and a procedure for the estimation of alkalinity and total inorganic carbon from titration data, Deep Sea Research Part A. Oceanographic Research Papers, 28, 609-623, https://doi.org/10.1016/0198-0149(81)90121-7, 1981.

Duran-Matute, M., Gerkema, T., De Boer, G., Nauw, J., and Gräwe, U.: Residual circulation and freshwater transport in the Dutch Wadden Sea: a numerical modelling study, Ocean Science, 10, 611-632, 2014.

Elias, E. P., Van der Spek, A. J., Wang, Z. B., and De Ronde, J.: Morphodynamic development and sediment budget of the Dutch Wadden Sea over the last century, Netherlands Journal of Geosciences, 91, 293-310, https://doi.org/10.1017/S0016774600000457, 2012.

Faber, P. A., Evrard, V., Woodland, R. J., Cartwright, I. C., and Cook, P. L.: Pore-water exchange driven by tidal pumping causes alkalinity export in two intertidal inlets, Limnology and Oceanography, 59, 1749-1763, https://doi.org/10.4319/lo.2014.59.5.1749, 2014.

Friedlingstein, P., O'sullivan, M., Jones, M. W., Andrew, R. M., Gregor, L., Hauck, J., Le Quéré, C., Luijkx, I. T., Olsen, A., and Peters, G. P.: Global carbon budget 2022, Earth System Science Data, 14, 4811-4900, 2022.

Glavovic, B., Limburg, K., Liu, K., Emeis, K., Thomas, H., Kremer, H., Avril, B., Zhang, J., Mulholland, M., and Glaser, M.: Living on the Margin in the Anthropocene: engagement arenas for sustainability research and action at the ocean–land interface, Current Opinion in Environmental Sustainability, 14, 232-238, https://doi.org/10.1016/j.cosust.2015.06.003, 2015.

Grasshoff, K., Kremling, K., and Ehrhardt, M.: Methods of seawater analysis, John Wiley & Sons, 2009.

Gruber, N., Clement, D., Carter, B. R., Feely, R. A., Van Heuven, S., Hoppema, M., Ishii, M., Key, R. M., Kozyr, A., and Lauvset, S. K.: The oceanic sink for anthropogenic CO_2 from 1994 to 2007, Science, 363, 1193-1199, DOI: 10.1126/science.aau5153, 2019.

Hansen, H., and Koroleff, F.: Determination of nutrients. Methods of Seawater Analysis: Third, Completely Revised and Extended Edition. Grasshoff, K., Kremling, K., and Ehrhardt, M. (Eds.), Weinheim, Germany: Wiley-VCH Verlag GmbH, 2007.

Hoppema, J.: The distribution and seasonal variation of alkalinity in the southern bight of the North Sea and in the western Wadden Sea, Netherlands journal of sea research, 26, 11-23, https://doi.org/10.1016/0077-7579(90)90053-J, 1990.

Hoppema, J.: The oxygen budget of the western Wadden Sea, The Netherlands, Estuarine, Coastal and Shelf Science, 32, 483-502, https://doi.org/10.1016/0272-7714(91)90036-B, 1991.

Hoppema, J.: Carbon dioxide and oxygen disequilibrium in a tidal basin (Dutch Wadden Sea), Netherlands journal of sea research, 31, 221-229, https://doi.org/10.1016/0077-7579(93)90023-L, 1993.

Hu, X., and Cai, W. J.: An assessment of ocean margin anaerobic processes on oceanic alkalinity budget, Global Biogeochemical Cycles, 25, doi.org/10.1029/2010GB003859, 2011.

Huettel, M., Røy, H., Precht, E., and Ehrenhauss, S.: Hydrodynamical impact on biogeochemical processes in aquatic sediments, The Interactions between Sediments and Water: Proceedings of the 9th International Symposium on the Interactions between Sediments and Water, held 5–10 May 2002 in Banff, Alberta, Canada, 2003, 231-236,

Jahnke, R. A., Craven, D. B., and Gaillard, J.-F.: The influence of organic matter diagenesis on $CaCO_3$ dissolution at the deep-sea floor, Geochimica et Cosmochimica Acta, 58, 2799-2809, 1994.

Jensen, K., Jensen, M., and Kristensen, E.: Nitrification and denitrification in Wadden Sea sediments (Königshafen, Island of Sylt, Germany) as measured by nitrogen isotope pairing and isotope dilution, Aquatic Microbial Ecology, 11, 181-191, doi:10.3354/ame011181, 1996.

Keith, D. W., Ha-Duong, M., and Stolaroff, J. K.: Climate strategy with CO_2 capture from the air, Climatic Change, 74, 17-45, https://doi.org/10.1007/s10584-005-9026-x, 2006.

Kérouel, R., and Aminot, A.: Fluorometric determination of ammonia in sea and estuarine waters by direct segmented flow analysis, Marine Chemistry, 57, 265-275, https://doi.org/10.1016/S0304-4203(97)00040-6, 1997.

Kieskamp, W. M., Lohse, L., Epping, E., and Helder, W.: Seasonal variation in denitrification rates and nitrous oxide fluxes in intertidal sediments of the western Wadden Sea, Marine ecology progress series. Oldendorf, 72, 145-151, 1991.

Lewis, E., and Wallace, D.: Program developed for CO_2 system calculations, Environmental System Science Data Infrastructure for a Virtual Ecosystem, 1998.

Louters, T., and Gerritsen, F.: The Riddle of the Sands: A Tidal SystenVs Answer to a Rising Sea Level, report RIKZ-94.040 (isbn 90-369-0084-0), 1994.

Luff, R., and Moll, A.: Seasonal dynamics of the North Sea sediments using a three-dimensional coupled sediment–water model system, Continental Shelf Research, 24, 1099-1127, https://doi.org/10.1016/j.csr.2004.03.010, 2004.

Martin, W., and Sayles, F.: $CaCO_3$ dissolution in sediments of the Ceara Rise, western equatorial Atlantic, Geochimica et Cosmochimica Acta, 60, 243-263, https://doi.org/10.1016/0016-7037(95)00383-5, 1996.

Matthews, H. D., and Caldeira, K.: Stabilizing climate requires near-zero emissions, Geophysical research letters, 35, https://doi.org/10.1029/2007GL032388, 2008.

Mehrbach, C., Culberson, C., Hawley, J., and Pytkowicx, R.: Measurement of the apparent dissociation constants of carbonic acid in seawater at atmospheric pressure, Limnology and oceanography, 18, 897-907, https://doi.org/10.4319/lo.1973.18.6.0897, 1973.

Meister, P., Herda, G., Petrishcheva, E., Gier, S., Dickens, G. R., Bauer, C., and Liu, B.: Microbial Alkalinity Production and Silicate Alteration in Methane Charged Marine Sediments: Implications for Porewater Chemistry and Diagenetic Carbonate Formation, Geochemical Signals in Dynamic Sedimentary Systems Along Continental Margins, 2022.

Meybeck, M.: Global chemical weathering of surficial rocks estimated from river dissolved loads, American journal of science, 287, 401-428, 10.2475/ajs.287.5.401, 1987.

Middelburg, J. J., Soetaert, K., and Hagens, M.: Ocean alkalinity, buffering and biogeochemical processes, Reviews of Geophysics, 58, e2019RG000681, https://doi.org/10.1029/2019RG000681, 2020.

Neumann, A., van Beusekom, J. E., Holtappels, M., and Emeis, K.-C.: Nitrate consumption in sediments of the German Bight (North Sea), Journal of Sea Research, 127, 26-35, 2017.

Norbisrath, M., Pätsch, J., Dähnke, K., Sanders, T., Schulz, G., van Beusekom, J. E., and Thomas, H.: Metabolic alkalinity release from large port facilities (Hamburg, Germany) and impact on coastal carbon storage, Biogeosciences, 19, 5151-5165, https://doi.org/10.5194/bg-19-5151-2022, 2022.

Norbisrath, M., Neumann, A., Dähnke, K., Sanders, T., Schöl, A., van Beusekom, J. E., and Thomas, H.: Alkalinity and nitrate dynamics reveal dominance of anammox in a hyper-turbid estuary, Biogeosciences, 20, 4307–4321, https://doi.org/10.5194/bg-20-4307-2023, 2023.

Pätsch, J.: Daily Loads of Nutrients, Total Alkalinity, Dissolved Inorganic Carbon and Dissolved Organic Carbon of the European Continental Rivers for the Years 1977 – 2022. 2024.

Petersen, W., Schroeder, F., and Bockelmann, F.-D.: FerryBox-Application of continuous water quality observations along transects in the North Sea, Ocean Dynamics, 61, 1541-1554, https://doi.org/10.1007/s10236-011-0445-0, 2011.

Postma, H.: Hydrography of the Dutch Wadden sea, Arch. Neerl. Zool, 10, 405-511, 1954.

Renforth, P., and Henderson, G.: Assessing ocean alkalinity for carbon sequestration, Reviews of Geophysics, 55, 636-674, https://doi.org/10.1002/2016RG000533, 2017.

Ridderinkhof, H., Zimmerman, J., and Philippart, M.: Tidal exchange between the North Sea and Dutch Wadden Sea and mixing time scales of the tidal basins, Netherlands Journal of Sea Research, 25, 331-350, https://doi.org/10.1016/0077-7579(90)90042-F, 1990.

Røy, H., Lee, J. S., Jansen, S., and de Beer, D.: Tide-driven deep pore-water flow in intertidal sand flats, Limnology and oceanography, 53, 1521-1530, https://doi.org/10.4319/lo.2008.53.4.1521, 2008.

Rutgers van der Loeff, M.: Transport van reactief silikaat uit Waddenzee sediment naar het bovenstaande water, NIOZ-rapport, 1974.

Sabine, C. L., Feely, R. A., Gruber, N., Key, R. M., Lee, K., Bullister, J. L., Wanninkhof, R., Wong, C., Wallace, D. W., and Tilbrook, B.: The oceanic sink for anthropogenic CO_2, science, 305, 367-371, DOI: 10.1126/science.1097403, 2004.

Santos, I. R., Chen, X., Lecher, A. L., Sawyer, A. H., Moosdorf, N., Rodellas, V., Tamborski, J., Cho, H.-M., Dimova, N., and Sugimoto, R.: Submarine groundwater discharge impacts on coastal nutrient biogeochemistry, Nature Reviews Earth & Environment, 2, 307-323, https://doi.org/10.1038/s43017-021-00152-0, 2021.

Schwichtenberg, F., Callies, U., and van Beusekom, J. E.: Residence times in shallow waters help explain regional differences in Wadden Sea eutrophication, Geo-Marine Letters, 37, 171-177, https://doi.org/10.1007/s00367-016-0482-2, 2017.

Schwichtenberg, F., Pätsch, J., Böttcher, M. E., Thomas, H., Winde, V., and Emeis, K.-C.: The impact of intertidal areas on the carbonate system of the southern North Sea, Biogeosciences, 17, 4223-4245, https://doi.org/10.5194/bg-17-4223-2020, 2020.

Shadwick, E., Thomas, H., Gratton, Y., Leong, D., Moore, S., Papakyriakou, T., and Prowe, A.: Export of Pacific carbon through the Arctic Archipelago to the North Atlantic, Continental Shelf Research, 31, 806-816, https://doi.org/10.1016/j.csr.2011.01.014, 2011.

Suchet, P. A., and Probst, J.-L.: Modelling of atmospheric CO_2 consumption by chemical weathering of rocks: application to the Garonne, Congo and Amazon basins, Chemical Geology, 107, 205-210, DOI:10.1016/0009-2541(93)90174-H, 1993.

Thomas, H., Bozec, Y., Elkalay, K., and De Baar, H. J.: Enhanced open ocean storage of CO_2 from shelf sea pumping, Science, 304, 1005-1008, DOI: 10.1126/science.1095491, 2004.

Thomas, H., Schiettecatte, L.-S., Suykens, K., Koné, Y., Shadwick, E., Prowe, A. F., Bozec, Y., de Baar, H. J., and Borges, A.: Enhanced ocean carbon storage from anaerobic alkalinity generation in coastal sediments, Biogeosciences, 6, 267-274, https://doi.org/10.5194/bg-6-267-2009, 2009.

van Bennekom, A., Krijgsman-van Hartingsveld, E., van der Veer, G., and van Voorst, H.: The seasonal cycles of reactive silicate and suspended diatoms in the Dutch Wadden Sea, Netherlands Journal of Sea Research, 8, 174-207, https://doi.org/10.1016/0077-7579(74)90016-7, 1974.

van Beusekom, J., Brockmann, U., Hesse, K.-J., Hickel, W., Poremba, K., and Tillmann, U.: The importance of sediments in the transformation and turnover of nutrients and organic matter in the Wadden Sea and German Bight, Deutsche Hydrografische Zeitschrift, 51, 245-266, 10.1007/BF02764176, 1999.

van Beusekom, J., and De Jonge, V.: Long-term changes in Wadden Sea nutrient cycles: importance of organic matter import from the North Sea, in: Nutrients and Eutrophication in Estuaries and Coastal Waters, Springer, 185-194, 2002.

van Beusekom, J. E., Buschbaum, C., and Reise, K.: Wadden Sea tidal basins and the mediating role of the North Sea in ecological processes: scaling up of management?, Ocean & coastal management, 68, 69-78, https://doi.org/10.1016/j.ocecoaman.2012.05.002, 2012.

van Beusekom, J. E., Carstensen, J., Dolch, T., Grage, A., Hofmeister, R., Lenhart, H., Kerimoglu, O., Kolbe, K., Pätsch, J., and Rick, J.: Wadden Sea Eutrophication: long-term trends and regional differences, Frontiers in Marine Science, 6, 370, doi.org/10.3389/fmars.2019.00370, 2019.

van der Zee, C., and Chou, L.: Seasonal cycling of phosphorus in the Southern Bight of the North Sea, Biogeosciences, 2, 27-42, https://doi.org/10.5194/bg-2-27-2005, 2005.

van Raaphorst, W., and van der Veer, H. W.: The phosphorus budget of the Marsdiep tidal basin (Dutch Wadden Sea) in the period 1950–1985: importance of the exchange with the North Sea, in: North Sea—Estuaries Interactions, Springer, 21-38, 1990.

Voynova, Y. G., Petersen, W., Gehrung, M., Aßmann, S., and King, A. L.: Intertidal regions changing coastal alkalinity: The Wadden Sea-North Sea tidally coupled bioreactor, Limnology and Oceanography, 64, 1135-1149, 2019.

Wang, Z. A., Kroeger, K. D., Ganju, N. K., Gonneea, M. E., and Chu, S. N.: Intertidal salt marshes as an important source of inorganic carbon to the coastal ocean, Limnology and Oceanography, 61, 1916-1931, 2016.

Waska, H., and Kim, G.: Submarine groundwater discharge (SGD) as a main nutrient source for benthic and water-column primary production in a large intertidal environment of the Yellow Sea, Journal of Sea Research, 65, 103-113, https://doi.org/10.1016/j.seares.2010.08.001, 2011.

Wolf-Gladrow, D. A., Zeebe, R. E., Klaas, C., Körtzinger, A., and Dickson, A. G.: Total alkalinity: The explicit conservative expression and its application to biogeochemical processes, Marine Chemistry, 106, 287-300, https://doi.org/10.1016/j.marchem.2007.01.006, 2007.

Wu, Z., Zhou, H., Zhang, S., and Liu, Y.: Using ^{222}Rn to estimate submarine groundwater discharge (SGD) and the associated nutrient fluxes into Xiangshan Bay, East China Sea, Marine pollution bulletin, 73, 183-191, https://doi.org/10.1016/j.marpolbul.2013.05.024, 2013.

Zalasiewicz, J., Williams, M., Steffen, W., and Crutzen, P.: The new world of the Anthropocene. ACS Publications, 2010.

Zhang, C., Shi, T., Liu, J., He, Z., Thomas, H., Dong, H., Rinkevich, B., Wang, Y., Hyun, J.-H., and Weinbauer, M.: Eco-engineering approaches for ocean negative carbon emission, Science Bulletin, 67, 2564-2573, https://doi.org/10.1016/j.scib.2022.11.016, 2022.

729